HAL
open science

Intrachromosomal mitotic non-allelic homologous recombination is the major molecular mechanism underlying type-2 NF1 deletions

Angelika C. Roehl, Julia Vogt, Tanja Mussotter, Antje Zickler, Helene Spoeri, Josef Hoegel, Nadia Chuzhanova, Katharina Wimmer, Lan Kluwe, Victor Mautner, et al.

To cite this version:

Angelika C. Roehl, Julia Vogt, Tanja Mussotter, Antje Zickler, Helene Spoeri, et al.. Intrachromosomal mitotic non-allelic homologous recombination is the major molecular mechanism underlying type-2 NF1 deletions. Human Mutation, 2010, 31 (10), pp.1163. 10.1002/humu.21340 . hal-00599473

HAL Id: hal-00599473

https://hal.science/hal-00599473v1

Submitted on 10 Jun 2011

HAL is a multi-disciplinary open access archive for the deposit and dissemination of scientific research documents, whether they are published or not. The documents may come from teaching and research institutions in France or abroad, or from public or private research centers.

L'archive ouverte pluridisciplinaire **HAL**, est destinée au dépôt et à la diffusion de documents scientifiques de niveau recherche, publiés ou non, émanant des établissements d'enseignement et de recherche français ou étrangers, des laboratoires publics ou privés.

Human Mutation

Intrachromosomal mitotic non-allelic homologous recombination is the major molecular mechanism underlying type-2 NF1 deletions

Journal:	*Human Mutation*
Manuscript ID:	humu-2010-0210.R2
Wiley - Manuscript type:	Research Article
Date Submitted by the Author:	27-Jul-2010
Complete List of Authors:	Roehl, Angelika; University of Ulm, Human Genetics Vogt, Julia; University of Ulm, Human Genetics Mussotter, Tanja; University of Ulm, Human Genetics Zickler, Antje; University of Ulm, Human Genetics Spoeri, Helene; University of Ulm, Human Genetics Hoegel, Josef; University of Ulm, Human Genetics Chuzhanova, Nadia; School of Science and Technology, Nottingham Trent University Wimmer, Katharina; Medical University Innsbruck, Medical Genetics Section, Department of Medical Genetics, Molecular and Clinical Pharmacology Kluwe, Lan; University Medical Center Hamburg-Eppendorf, Maxillofacial Surgery Mautner, Victor; University Hospital Eppendorf, Maxillofacial Surgery Cooper, David; Cardiff University, Institute of Medical Genetics, College of Medicine Kehrer-Sawatzki, Hildegard; University of Ulm, Human Genetics
Key Words:	mitotic non-allelic homologous recombination , Neurofibromatosis type 1 , genomic disorders, non-B DNA, parental and chromosomal origin, recombination hotspot, microdeletions

SCHOLARONE™
Manuscripts

Intrachromosomal mitotic non-allelic homologous recombination is the major molecular mechanism underlying type-2 *NF1* deletions

Angelika C. Roehl[1], Julia Vogt[1], Tanja Mussotter[1], Antje N. Zickler[1], Helene Spöri[1], Josef Högel[1], Nadia A. Chuzhanova[2], Katharina Wimmer[3], Lan Kluwe[4], Victor-Felix Mautner[4], David N. Cooper[5], Hildegard Kehrer-Sawatzki[1]

[1] Institute of Human Genetics, University of Ulm, Albert-Einstein-Allee 11, Ulm, Germany

[2] School of Science and Technology, Nottingham Trent University, Clifton Lane, Nottingham NG11 8NS, UK

[3] Division of Human Genetics, Medical University Innsbruck, Innsbruck, Austria

[4] Department of Maxillofacial Surgery, University Medical Centre, Hamburg-Eppendorf, Germany

[5] Institute of Medical Genetics, School of Medicine, Cardiff University, Cardiff CF14 4XN, UK

Corresponding author:

Hildegard Kehrer-Sawatzki

Institute of Human Genetics, University of Ulm

Albert-Einstein-Allee 11, 89081 Ulm, Germany

Phone: 0049 731 50065421, FAX: 0049 731 50065402

Email: hildegard.kehrer-sawatzki@uni-ulm.de

For Peer Review

Key Words: Neurofibromatosis type 1 (NF1), mitotic non-allelic homologous recombination (NAHR), microdeletion, parental and chromosomal origin, genomic disorders, recombination hotspot, tumorigenesis, *Alu* sequences, non-B DNA

For Peer Review

Abstract

Non-allelic homologous recombination (NAHR) is responsible for the recurrent rearrangements that give rise to genomic disorders. Although meiotic NAHR has been investigated in multiple contexts, much less is known about mitotic NAHR despite its importance for tumorigenesis. Since type-2 *NF1* microdeletions frequently result from mitotic NAHR, they represent a good model in which to investigate the features of mitotic NAHR. We have used microsatellite analysis and SNP arrays to distinguish between the various alternative recombinational possibilities, thereby ascertaining that 17 of 18 type-2 *NF1* deletions, with breakpoints in the *SUZ12* gene and its highly homologous pseudogene, originated via intrachromosomal recombination. This high proportion of intrachromosomal NAHR causing somatic type-2 *NF1* deletions contrasts with the interchromosomal origin of germline type-1 *NF1* microdeletions, whose breakpoints are located within the NF1-REPs (low-copy repeats located adjacent to the *SUZ12* sequences). Further, meiotic NAHR causing type-1 *NF1* deletions occurs within recombination hotspots characterized by high GC-content and DNA duplex stability, whereas the type-2 breakpoints associated with the mitotic NAHR events investigated here do not cluster within hotspots and are located within regions of significantly lower GC-content and DNA stability. Our findings therefore point to fundamental mechanistic differences between the determinants of mitotic and meiotic NAHR.

For Peer Review

Introduction

Genomic disorders result from microdeletions or microduplications of several hundred kilobases whose formation is mediated by the local DNA sequence architecture, in particular region-specific low-copy repeats (LCRs) or segmental duplications [Shaw and Lupski, 2004; Lupski, 2009; Mefford and Eichler, 2009; Zhang et al., 2009a; Carvalho et al., 2010]. Recurrent microdeletions and their reciprocal microduplications are caused predominantly by non-allelic homologous recombination (NAHR) [Gu et al., 2008; Stankiewicz and Lupski, 2010]. The molecular mechanisms underlying NAHR are assumed to be similar to those of allelic homologous recombination (AHR), but, instead of an allelic homologous template, NAHR employs a similar yet non-allelic template to repair the initiating double strand break (DSB) [Steele et al., 1991; Hurles and Lupski, 2006; Sasaki et al., 2010]. Homologous recombination (HR) is in general a very precise repair mechanism for DNA lesions such as DSBs [Mao et al., 2008]. Thus, no 'scars' of the DSB-repair process, such as small insertions or deletions, are apparent at the breakpoint junctions repaired by HR, as they often are at the breakpoints of DNA lesions repaired by non-homologous end-joining (NHEJ) [Lieber, 2010]. Chromosomal regions harbouring multiple duplicated sequences, such as the *NF1* gene region, are inherently prone to recurrent NAHR-mediated rearrangements. By contrast, non-recurrent rearrangements tend to be mediated by NHEJ or by replication-based mechanisms such as 'fork stalling and template switching' (FoSteS) [Lee et al., 2007; Vissers et al., 2009; Zhang et al., 2009b]. Although the breakpoint regions of non-recurrent chromosomal rearrangements do not exhibit extensive sequence similarity, they often occur close to LCRs [Shaw et al., 2004; Lupski and Stankiewicz, 2005; Bauters et al., 2008; Zhang et al., 2010]. This suggests that the unusual genome architecture associated with LCRs may serve to 'confuse' the DNA replication machinery resulting in replication errors that generate breakpoints which in turn lead to complex genomic rearrangements [Lee et al., 2007; Hastings et al., 2009; Zhang et al., 2009b, 2009c].

Deleted: between LCRs

For Peer Review

Large deletions in the *NF1* gene region at 17q11.2 (MIM# 613113) belong to the abovementioned group of genomic disorders [Jenne et al., 2003; Forbes et al., 2004]. Two common types of recurrent *NF1* deletion have been identified which differ in terms of their size and breakpoint location: type-1 *NF1* deletions span 1.4-Mb and are mediated by NAHR between LCRs termed NF1-REP A and NF1-REP C [Dorschner et al., 2000; Jenne et al., 2001; Lopez-Correa et al., 2001]. The majority of type-1 *NF1* deletions are maternally inherited germ-line deletions [Upadhyaya et al., 1998; López-Correa et al., 2000; Steinmann et al., 2008] whose breakpoints are located within two hotspot regions of meiotic recombination termed PRS1 and PRS2 [López-Correa et al., 2001; Forbes et al., 2004]. By contrast, type-2 *NF1* deletions encompass only 1.2-Mb and their breakpoints are located within the *SUZ12* gene (MIM# 606245) and its pseudogene *SUZ12P* which immediately flank the NF1-REPs (Fig. 1). In individuals with type-2 *NF1* deletions, somatic mosaicism with normal cells is frequently observed, indicating an early postzygotic (mitotic) origin for these deletions [Petek et al., 2003; Kehrer-Sawatzki et al., 2004; Steinmann et al., 2007]. Whereas an estimated 70% of all *NF1* deletions are type-1, only 10-20% are type-2 which are therefore much less frequently encountered than the germline type-1 *NF1* deletions [Kehrer-Sawatzki et al., 2004].

Although NAHR is a major cause of genome instability in humans, the underlying molecular mechanisms are not well understood. Different types of NAHR have been observed that are distinguishable by virtue of the chromosomal origin of the resulting rearrangements, in other words whether they have arisen via inter- or intra-chromosomal NAHR [reviewed by Gu et al., 2008]. The chromosomal origins of the various deletions or duplications known to be responsible for genomic disorders have been generally ascertained by microsatellite marker analysis [Thomas et al., 2006 and references therein]. Although type-1 *NF1* deletions have previously been shown to arise by interchromosomal NAHR during maternal meiosis I [López-Correa et al., 2000], much less is known about the chromosomal origin and

Deleted: , their occurrence being strongly influenced by the local genomic architecture

Deleted: however

Deleted: ; Steinmann et al., 2008

For Peer Review

underlying generative mechanism of type-2 *NF1* deletions. Until now, only four type-2 deletions had been analysed in terms of their chromosomal origin [Steinmann et al., 2007]. In this study, we have used microsatellite markers and SNP arrays to characterize 14 additional type-2 *NF1* deletions in order to acquire insight into the molecular mechanism(s) underlying these unusual somatic deletions. Our study has demonstrated that SNP array analysis represents a valuable tool not only to characterize genomic rearrangements such as microdeletions and microduplications, but also to determine their chromosomal origin. In addition, comparative analysis of type-1 and type-2 deletion breakpoint junctions revealed substantial differences in terms of the precise locations and DNA sequence characteristics of the microdeletion breakpoints that appear to be suggestive of basic mechanistic differences between NAHR events depending upon whether they have occurred during meiosis or during early postzygotic/mitotic cell divisions.

Deleted: Petek et al., 2003; Kehrer-Sawatzki et al., 2004;

For Peer Review

Patients, Materials and Methods

Patients and deletion breakpoint identification

In this study, we have investigated the mechanisms underlying 18 type-2 *NF1* deletions. The precise breakpoints of 13 of the 18 type-2 deletions studied here have been previously described [Kehrer-Sawatzki et al., 2004; Steinmann et al., 2007]. The breakpoints of 5 newly identified type-2 *NF1* deletions were characterized in this study employing the methods summarized in Supp. Table S1. The sequences of the PCR primers used to identify the breakpoints are available from the authors upon request. The clinical features of these 5 newly identified patients with type-2 *NF1* deletions are summarized in Supp. Table S2.

Search for the reciprocal duplication

In order to search for duplications reciprocal to the somatic deletions observed in patients with type-2 *NF1* deletions mediated by NAHR, we performed duplication-specific

breakpoint-spanning PCRs with forward primers designed to bind specifically to the *SUZ12* sequence, and a reverse primer specific for the *SUZ12P* sequence according to the assay principle described by Turner et al. [2008] (Supp. Table S3). PCR reactions with paralog-specific primers were performed using genomic DNA isolated from peripheral blood of the patients and Platinum Taq polymerase (Invitrogen).

Analysis of somatic mosaicism

Mosaicism for cells with and without the deletion was investigated in the 5 newly identified type-2 *NF1* deletions characterized in this study. To this end, FISH analysis was performed on primary blood lymphocytes cultivated for 72h with phytohaemagglutinin. In each case, at least 200 blood cells were evaluated by interphase FISH. FISH analysis was not performed on whole blood cell populations without cultivation. If buccal cells were available for FISH analysis, ~100 interphase nuclei were evaluated. Mosaicism was also investigated by microsatellite marker analysis of DNA isolated from peripheral blood samples and buccal swabs as described [Kehrer-Sawatzki et al., 2004]. The results of the mosaicism analysis in all 18 patients with type-2 *NF1* deletions so far characterized by ourselves are summarized in (Supp. Table S4).

In order to investigate potential mosaicism for the type-2 deletion in peripheral blood samples taken from the parents of patients 2358 and 2429, deletion-specific breakpoint-spanning PCR was performed. The primers used for these assays bind to sites of paralogous sequence variants (PSVs) between *SUZ12* and *SUZ12P*. Using such specific primer combinations, only the deletion-specific breakpoint-spanning fragments are amplified by PCR and not sequences that derive from *SUZ12* or *SUZ12P* on the wild-type chromosome 17. The primer sequences used to PCR amplify across the deletion breakpoints of patients 2358 and 2429 are available on request.

For Peer Review

Microsatellite marker analysis

Polymorphic microsatellite markers located on chromosome 17 were investigated to determine the chromosomal origin of the deletions, viz. whether the deletions originated via intrachromosomal or interchromosomal recombination. Four of the eighteen deletions (those of patients IL-39, KCD, HC and 697) were previously analysed by this method [Steinmann et al., 2007], whereas 14 patients were investigated for the first time here (Supp. Fig. S1). The parental origin of each chromosome 17 carrying a deletion was also determined. To this end, DNA from all patients was investigated together with DNA from their parents and, if available, their siblings. Genomic DNA was extracted either from venous blood, from buccal swabs or from saliva as indicated in Supp. Fig. S1. Microsatellite markers were also genotyped using DNA extracted from human/mouse somatic cell hybrids containing either the deletion-bearing or the wild-type chromosome 17 of the patient (Supp. Fig. S1). Primer sequences used to PCR-amplify microsatellite markers are available from the authors on request.

SNP array analysis

Sixteen of the 18 patients harbouring somatic type-2 *NF1* deletions were genotyped by means of the Human SNP arrays 6.0 (Affymetrix, St. Clara, CA) using DNA extracted from peripheral blood lymphocytes from the patients as previously described [Roehl et al., 2010; Supp. Table S5].

Bioinformatic and statistical analysis

Sequences spanning the breakpoint (recombination) regions of the 16 type-2 *NF1* deletions mediated by NAHR were screened for the presence of 109 different DNA sequence motifs (and their complements) of length ≥5 nucleotides (nt) which have been reported to be associated with DNA breakage, repair and recombination [Cullen et al., 2002; Abeysinghe et

For Peer Review

al., 2003; Ball et al., 2005; Myers et al., 2008; Chuzhanova et al., 2009; Makridakis et al., 2009]. A similar analysis was performed in our previous study [Steinmann et al., 2007] but this time the number of recombination-associated motifs investigated was increased from 37 to 109, since in the meantime many more recombination-associated motifs have been identified. In addition, both the actual recombination regions and 100 nt segments flanking them on either side, were analysed by complexity analysis [Gusev et al., 1999] in order to identify direct, inverted and symmetric repeats ≥ 6 nt separated by no more than 20 bp. Such repeats are capable of non-B DNA formation, in particular slipped, cruciform and triplex structures [Wells, 2007].

For each of the above searches, the statistical significance of our findings was assessed by comparison with 1000 control datasets using z-score statistics [as described in Chuzhanova et al., 2009]. Two regions of chromosome 17, flanking the *NF1* gene but not including any of the known recombination hotspots, were used to generate matching control datasets: [coordinates 26,109,477 to 26,359,000 (centromeric to the *NF1* gene, between but not including either *SUZ12P* or the NF1-REPs A and B) and 26,889,356 to 27,203,003 (telomeric to the *NF1* gene up to, but not including either *SUZ12* or NF1-REP C); human genome assembly hg18 (NCBI build 36)].

The GC-content of the deletion breakpoint regions was determined using RepeatMasker (http://www.repeatmasker.org/cgi-bin/WEBRepeatMasker) and a program provided by EnCor Biotechnology Inc. (http://www.encorbio.com/protocols/Nuc-MW.htm).

The potential clustering of type-2 deletion breakpoints mediated by NAHR was assessed by means of the Kolmogorov-Smirnov-test, comparing the distribution function $F_N(X)$ of the breakpoint localizations within the *SUZ12* gene identified in the patients with a theoretical uniform distribution.

DNA stability

For Peer Review

DNA helix stability was determined by calculating the average dissociation free energy (ΔG°) of each overlapping dinucleotide according to the method described by Breslauer et al. [1986].

Results

Deletion breakpoint localization

We initiated this study by identifying the breakpoints of five previously uncharacterized type-2 *NF1* deletions. Utilizing paralogous sequence variants (PSVs) to differentiate between the *SUZ12* gene and its pseudogene, the breakpoint regions were identified with the highest possible resolution and assigned to recombination regions (RRs) of between 64 bp and 225 bp (Table 1; patients 2358, 585, 1956, 2429, UC172). These RRs represent segments of absolute sequence identity between *SUZ12* and *SUZ12P* and must contain the deletion breakpoints themselves. NAHR is the mechanism underlying all five newly characterized type-2 *NF1* deletions since the breakpoints were identified at homologous sites between *SUZ12* and *SUZ12P*. The breakpoint data from these five newly characterized type-2 deletions were then combined with the breakpoint data from 13 previously reported cases [Steinmann et al., 2007] in order to make a general assessment of the molecular mechanism underlying type-2 *NF1* deletions.

Deleted: was deemed to be

Deleted: most likely

Recombinational mechanism underlying type-2 NF1 deletions

Non-allelic homologous recombination (NAHR) was responsible for the type-2 deletions in 16 of the 18 NF1 patients analysed (Table 1). In only two of the 18 patients studied (patients HC and 928) were the deletion breakpoints not located at homologous sites within *SUZ12* and *SUZ12P* [Steinmann et al., 2007].

Deleted: , since the deletion breakpoints were found to be located at homologous sites within the *SUZ12* gene and its pseudogene *SUZ12P*. Indeed, NAHR appears to be the major mechanism responsible for type-2 *NF1* deletions (Table 1) since

Deleted: i

Deleted: Kehrer-Sawatzki et al., 2004;

Somatic mosaicism

For Peer Review

Somatic mosaicism of cells with and without the type-2 *NF1* deletion was noted in 3 of the 5 newly identified patients with type-2 deletions. Taken together with the results of our previous analysis on mosaicism in patients with type-2 *NF1* deletions [Steinmann et al., 2007], 16 of the 18 patients studied exhibited somatic mosaicism, indicative of an early postzygotic/mitotic origin for the deletions (Supp. Table S4).

In two patients (2429 and 2358), neither FISH performed on primary blood samples, nor microsatellite marker analysis using DNA from buccal swabs, provided any hint as to the presence of normal cells lacking the *NF1* deletion. In addition, neither breakpoint-spanning PCR with primers designed to amplify across the deletion breakpoints, nor FISH analysis of peripheral blood samples, revealed any evidence of low-level mosaicism for the respective deletions in the parents of these patients. The 16 year-old male patient 2429 presented with a severe clinical phenotype characterized by multiple cutaneous and subcutaneous neurofibromas, an MPNST and dysmorphic facial features (Supp. Table S2). The severe manifestations of NF1 exhibited by patient 2429 are consistent with the conclusion that he possesses a *de novo* germline type-2 *NF1* deletion.

Female patient 2358 was 10 years old at the time of investigation and had multiple café-au-lait spots, mild facial dysmorphism, mild developmental delay and a plexiform neurofibroma. Although it is very likely that patient 2358 possesses a *de novo* germline type-2 *NF1* deletion, we were unable to confirm this postulate by skin biopsy analysis since it was declined by the parents of patient 2358.

Chromosomal origin of the type-2 NF1 deletions mediated by NAHR

NAHR causing 16 of the 18 type-2 *NF1* deletions under investigation is initiated by the misalignment of the *SUZ12* and *SUZ12P* sequences which exhibit 96.2% similarity over their shared 45 kb lengths. In principle, NAHR could occur within a chromatid, between sister-chromatids or between chromosomes, at different stages during the cell cycle. Thus,

Deleted: (intrachromosomal NAHR)

Deleted: (interchromosomal NAHR)

Deleted: Moreover, NAHR can occur

For Peer Review

intrachromosomal NAHR during G1-phase, which has been found to occur in mammalian cells [Stanfield and Helinski, 1984], would be expected to give rise to a deletion plus an excised circular DNA (Fig. 2A). By contrast, intrachromosomal NAHR post-replication may occur either within one chromatid (intrachromatid NAHR) or between sister chromatids (interchromatid NAHR) (Fig. 2B). Finally, interchromosomal NAHR may occur between non sister-chromatids either in G1-phase (Fig. 3A) or post-replication (Fig. 3B). Depending upon the stage in the cell cycle, the chromosomal consequences of NAHR will be very different. When NAHR occurs between chromosomes, the deletion-causing NAHR event would be expected to give rise to sequence homozygosity distal to the deletion (Fig. 3B). Interchromosomal (allelic) homologous recombination does indeed occur in somatic cells and leads to loss of heterozygosity (LOH) which is a common cause of tumorigenesis [Hagstrom and Dryja, 1999; Howarth et al., 2009] and has been well documented in NF1-associated tumours [Serra et al., 2010; Stephens et al., 2006; Upadhyaya et al., 2009; Steinmann et al., 2009; Garcia-Linares et al., 2010]. In order to investigate the presence of extended regions of homozygosity encompassing the majority of 17q distal to the *NF1* type-2 deletions, which would be indicative of the deletions having resulted from interchromosomal NAHR, we evaluated SNP array results for the 16 patients in whom it could be established that the somatic deletions had been mediated by NAHR. The use of SNP arrays to detect somatic loss of heterozygosity was used here for the first time to ascertain the chromosomal origin of type-2 *NF1* deletions.

In our previous study, SNP arrays were used to analyse runs of homozygosity (ROHs) in the *NF1* gene and its immediate flanking regions [Roehl et al., 2010]. However, in the context of the present study, these SNP array data acquired new utility by helping to determine the presence or absence of an extended region of homozygosity encompassing the majority of chromosome 17q distal to the type-2 *NF1* deletions. The presence of homozygosity extending over many Mb of 17q would have suggested that interchromosomal NAHR had caused these

Deleted: occurring within one chromosome

Deleted: before replication

Deleted: at which the NAHR event occurs

Deleted: in somatic cells

Deleted: the presence or absence of

Deleted: provided strong support for the contention

For Peer Review

deletions. However, evaluation of the SNP array data for the complete set of SNPs on chromosome 17 served to exclude the occurrence of extended regions of homozygosity distal to the *NF1* deletions. Only short ROHs (between 202 kb and 568 kb in length) immediately flanking the type-2 *NF1* deletions in a telomeric direction were noted (Supp. Table S6, Fig. 4). It is most unlikely that these ROHs had originated via interchromosomal recombination events mediating the *NF1* deletions since similarly sized ROHs (between 200 kb and 600 kb) were also observed in 41 of 60 CEU individuals evaluated as controls [Roehl et al., 2010; Supp. Table S7]. Since the prevalence of ROHs ranging in size from 200 to 600 kb turned out not to be significantly different in patients with type-2 *NF1* deletions as compared with CEU controls ($p = 0.37$; two-tailed Fisher's Exact test), we concluded that the 16 type-2 *NF1* deletions were not generated via interchromosomal NAHR because this mechanism would have given rise to extended regions of homozygosity on 17q. Instead, the 16 deletions were considered to have been caused by intrachromosomal NAHR. To confirm this initial assessment, we performed microsatellite marker analysis using DNA from the patients and their family members as well as DNA from human/mouse somatic cell hybrids containing either the wild-type or the deletion-containing chromosome 17 from the respective patients (Supp. Fig. S1). This analysis indicated that 17 of the 18 type-2 *NF1* deletions originated from intrachromosomal recombination. Only in one of the 18 patients, patient 2429, was the type-2 deletion probably caused by interchromosomal NAHR during paternal meiosis since this was the most likely mechanism to account for the observed haplotypes (Supp. Fig. S1-N, Table 2). FISH analysis of primary blood lymphocytes failed to yield any evidence for somatic mosaicism for the deletion in either patient 2429 (Supp. Table S4) or his parents. Deletion breakpoint-specific PCR assays did not detect the deletion in peripheral blood samples of the parents of patient 2429. We therefore concluded that this patient possesses a *de novo* germline type-2 *NF1* deletion.

For Peer Review

In 13 of the 18 type-2 *NF1* deletions investigated, we were able to establish unequivocally whether the deletion had occurred on the paternal or maternal chromosome 17. Four deletions were found to have occurred on the paternal chromosome whereas 9 deletions had occurred on the maternal chromosome (Table 2). Hence, there was no significant preference for the deletions to occur on either the maternal or paternal chromosome ($p = 0.267$; two-sided exact version of the goodness-of-fit χ^2-test).

As schematically depicted in Figure 2B, intrachromosomal NAHR between sister-chromatids should in principle also yield cells harbouring duplications reciprocal to the deletions. In order to search for these reciprocal duplications, we performed breakpoint-spanning PCR with forward primers designed to bind specifically to the *SUZ12* sequence, and a reverse primer specific for the *SUZ12P* sequence according to the assay principle described by Turner et al. [2008] (Supp. Table S3). However, no such reciprocal duplications were detected in DNA isolated from the primary blood samples of any of the patients with type-2 *NF1* deletions.

Analysis of a possible clustering of type-2 NF1 deletion breakpoints

Meiotic recombination hotspots have been identified that are confined to genomic regions of between ~500 bp and ~4 kb [Reiter et al., 1998; Lopez-Correa et al., 2001; Kauppi et al., 2004; Paigen and Petkov, 2010]. Much less is however known about the existence of mitotic recombination hotspots in general. Using our combined dataset of a total of 16 type-2 deletions of postzygotic origin, we did not identify any significant clustering of breakpoints in the patients tested (Kolmogorov-Smirnov-test, $p = 0.205$). Despite the general absence of breakpoint clusters, the deletion breakpoints in patients WB and UC172 were nevertheless found to occur within the same 177 bp interval (Fig. 1).

Structural features of the recombination regions which could have promoted NAHR

For Peer Review

The breakpoint regions of the 16 deletions mediated by NAHR were assigned by reference to the paralogous sequence variants (PSVs) which serve to distinguish *SUZ12* and *SUZ12P*. These breakpoint regions, also termed recombination regions (RRs), span between 46bp and 225 bp (as summarized in Table 1) and represent segments of absolute sequence identity between *SUZ12* and *SUZ12P*. Since the RRs must contain the deletion breakpoints, they were screened for the presence of known recombination-promoting motifs potentially involved in DNA breakage and repair. However, the only recombination-associated motif found to be overrepresented within the RRs as compared to a control dataset was the χ-like element (CCWCCWGC) and its complementary motif ($p < 0.05$). Although this motif was found to be overrepresented as compared with the control dataset, it was only observed in 2 of the 16 RRs examined (Supp. Table 8).

Deleted: should be stated that it

In addition to the above motif search, the RRs and extended RRs (which included additional 100 bp segments flanking the RRs on either side) were screened for the presence of repeats capable of mediating non-B DNA structure formation. Inverted repeats were found to be overrepresented within the RRs ($p < 0.001$) whereas both direct and inverted repeats were overrepresented within the extended RRs ($p < 0.001$) as compared to control datasets. Taken together, the RRs of 14 of the 16 deletions (88%) caused by NAHR were found to harbour short repeats capable of forming non-B DNA structures (Supp. Figure S2).

Prevalence of Alu elements within the recombination regions

The breakpoints of structural variants in the human genome, such as deletions and insertions mediated by NAHR, have been found to be disproportionately associated with SINE/*Alu* elements [Witherspoon et al., 2009; Lam et al., 2010]. Consistent with these findings, *Alu* elements were found to be significantly overrepresented at the type-2 deletion breakpoints as compared with the *Alu* frequency within the 45 kb segment of the *SUZ12* gene homologous to

For Peer Review

SUZ12P ($p < 0.0001$; exact goodness-of-fit χ^2 test) (Supp. Table S9). Indeed, 10 of the 16 type-2 *NF1* deletions mediated by NAHR actually overlapped with SINE/*Alu* elements.

DNA stability and GC content

In previous studies, breakpoint regions of structural variants generated by meiotic NAHR events have been found to be (i) biased towards GC-rich regions and (ii) to manifest higher DNA helix stability and lower DNA flexibility as compared with rearrangements caused by non-homologous end joining (NHEJ) [Lopes-Correa et al., 2001; Visser et al., 2005; Lam et al., 2010]. In order to permit comparison of the physical features of the breakpoints respectively associated with meiotic and mitotic NAHR events within the *NF1* gene region, DNA stability and GC-content were determined for both the mitotic type-2 deletion breakpoint regions characterized here, and the PRS1 and PRS2 hotspot regions of meiotic recombination which contain the type-1 *NF1* deletion breakpoints. Both the DNA stability and GC-content of the breakpoint regions of type-2 *NF1* deletions were found to be significantly lower than in the PRS1 and PRS2 hotspots ($p < 0.0001$, one-sample *t*-test; Supp. Tables S10, S11).

Discussion

In this study, we have employed a combination of SNP array and microsatellite marker analysis to determine the chromosomal origin of type-2 *NF1* microdeletions and to ascertain the underlying generational mechanism(s). Our analysis revealed that 17 of the 18 type-2 *NF1* deletions were generated by an intrachromosomal mechanism. Further, 16 of the 18 type-2 *NF1* deletions resulted from intrachromosomal NAHR, whereas the remaining two deletions exhibited breakpoints at non-homologous locations within *SUZ12* and *SUZ12P* (Tables 1 and 2). The postzygotic origin of 16 of the 17 type-2 deletions caused by intrachromosomal recombination was evidenced by the presence of mosaicism with normal cells without the

Deleted: for the first time

Deleted: not only

Deleted: but also

Deleted: unequal recombination between the highly homologous *SUZ12* and *SUZ12P* repeats.

For Peer Review

deletion (Supp. Table S4). Only one of the 18 type-2 *NF1* deletions under investigation, the deletion in patient 2429, was mediated by interchromosomal NAHR. In our view, it is unlikely to be a mere coincidence that this was also a documented case of *de novo* germline type-2 *NF1* deletion. Taken together, our findings indicate that type-2 *NF1* deletions of early postzygotic origin arise predominantly by intrachromosomal NAHR (Fig. 2). However, the occasionally encountered germline type-2 *NF1* deletion mediated by interchromosomal NAHR serves to demonstrate that meiotic recombination is feasible between *SUZ12* and *SUZ12P* even although it is infrequent.

Deleted: (most likely during paternal meiosis)

Whereas most type-2 *NF1* deletions are of postzygotic origin, the vast majority of type-1 *NF1* deletions with breakpoints located within the NF1-REPs A and C are mediated by interchromosomal NAHR during maternal meiosis [López-Correa et al., 2000; Steinmann et al., 2008]. This mirrors the origin of the germline microdeletions underlying Williams-Beuren syndrome, DiGeorge syndrome and Angelman syndrome which are also predominantly generated by interchromosomal NAHR during either maternal or paternal meiosis [Thomas et al., 2006 and references therein]. The predominance of interchromosomal NAHR events during meiosis may be related to the unique pairing of homologous chromosomes during synapsis, which differs quite radically from any chromosome pairing during the postzygotic cell cycle. Interchromosomal recombination during meiosis may be facilitated by the close synapsis between homologous chromosomes during the prophase of meiosis I, which in mammals lasts for many hours [Adler, 1996]. Synapsis is fully established at the zygotene stage of meiotic prophase I and involves the intimate association of homologues in the synaptonemal complex (SC) [reviewed in Roeder, 1997; Gerton and Hawley, 2005; Ding et al., 2010]. The SC appears to facilitate recombination between non-sister chromatids, as evidenced by the observation that yeast mutants which lack the ability to form SCs display a ~10-fold lower recombination rate [Rockmill and Roeder, 1990; Xu et al., 1997]. The pairing of homologous chromosomes in human somatic cells has been visualized by the

Deleted: ,

Deleted: whether allelic or non-allelic,

Deleted: However, at least in yeast, chromosome synapsis is not an absolute requirement for recombination to occur [Sym and Roeder, 1994; Storlazzi et al., 1996; Loidl, 2006; Ding et al., 2010].¶

For Peer Review

analysis of chromosome territories in interphase nuclei, although both inter-chromosome and tissue-specific differences in pairing frequency exist [Zeitz et al., 2009]. However, the pairing of homologous chromosomes during mammalian mitosis is probably different in nature and much less stable than the inter-homologue pairing within the meiotic SC [reviewed by Meaburn and Misteli, 2007]. Despite these surmised differences in chromosome pairing, observations made in yeast mitotic cells have suggested that meiotic and mitotic recombination are likely to share mechanistic similarities. In yeast, it has been shown that homologous recombination is mediated by joint molecule intermediates whose strand composition and size are identical to those of the canonical double Holliday junctions (DHJ) structures observed in yeast meiosis [Bzymek et al., 2010]. DHJs form preferentially between yeast sister chromatids during mitotic DSB repair whereas in meiosis a preference for inter-homologue recombination has been observed [Bzymek et al., 2010]. These observations are analogous to the situation we observe in humans in the context of *NF1* deletions: intrachromosomal NAHR is the major mechanism causing type-2 *NF1* deletions of postzygotic origin, whereas interchromosomal NAHR during maternal meiosis is responsible for the germline type-1 *NF1* deletions.

It is unclear at what point, during the cell cycle, intrachromosomal NAHR gives rise to type-2 *NF1* deletions. Most mitotic recombination events are likely to occur during G1-, S- or G2-phase rather than mitosis proper [LaFave and Sekelsky, 2009; Moynahan and Jasin, 2010]. The methods adopted in our study (SNP array and microsatellite marker analysis) did not allow us to ascertain whether the intrachromosomal NAHR events occurred in cells during G1-phase or post-replication. The outcomes of intrachromosomal NAHR in the different phases of the cell cycle can be quite diverse. If intrachromosomal NAHR were to have occurred between sister-chromatids (post-replication), then cells bearing the reciprocal duplication might also have arisen in addition to those cells harbouring the type-2 deletion (Fig. 2B). We therefore sought evidence for the presence of the duplication reciprocal to the

Deleted: involving the *NF1* gene region

Deleted: As indicated in Figure 2, t

For Peer Review

type-2 deletions by performing FISH on interphase blood cells and PCR on peripheral blood lymphocytes using primers specifically designed to PCR amplify across the predicted duplication breakpoints. In principle, this latter method should have been capable of detecting even small numbers of cells harbouring the duplication. This notwithstanding, we failed to detect the presence of any such duplication in the peripheral blood lymphocytes of patients in whom intrachromosomal NAHR had been established. It is possible that the putative duplication is not represented in the DNA isolated from peripheral blood cells. Even although no evidence for the presence of duplications was forthcoming in this study, we cannot exclude the possibility that post-replication recombination events caused the type-2 *NF1* deletions (Fig. 2B). In yeast mitotic cells, homologous recombination is largely confined to the S- and G2-phases. During these time periods, the sister chromatid is available to mediate DBS repair [Sjögren and Nasmyth, 2001; Krogh and Symington, 2004; Moynahan and Jasin, 2010]. Thus, we may also infer that type-2 *NF1* deletions are likely to have been generated by intrachromosomal NAHR between sister chromatids rather than within one chromatid. Analogous to this situation, intrachromosomal NAHR between sister chromatids has been shown to be the major mechanism underlying duplications at the α-globin locus in human blood cells [Lam and Jeffreys, 2007].

Allelic and non-allelic meiotic recombination events occur preferentially at specific hotspots, which are usually confined to regions of ~500 bp up to ~3–4 kb [Reiter et al., 1998; Lopez-Correa et al., 2001; Kauppi et al., 2004; Lupski, 2004; Kurotaki et al., 2005; Myers et al., 2005; Visser et al., 2005; De Raedt et al., 2006; Lindsay et al., 2006; Torres-Juan et al., 2007; Turner et al., 2008; Wu et al., 2010; Zhang et al., 2010; Paigen and Petkov, 2010]. Importantly, some NAHR hotspots have been shown to operate exclusively during meiosis and not during mitosis [Turner et al., 2008]. In the NF1 context, ~80% of all meiotic type-1 deletions display breakpoints located within the PRS1 and PRS2 hotspots, which span 2.9 kb and 3.5 kb, respectively [Forbes et al., 2004; De Raedt et al., 2006]. No such hotspot of

Deleted: it may well be that the

Deleted: responsible for

Deleted: occur post-replication

Deleted: Once again, we base this assumption upon observations made i

Deleted: in which

Deleted: for which cohesion between sister chromatids appears to be essential

Deleted: generally

Deleted: at all

For Peer Review

mitotic NAHR, confined to a few kilobases and occurring in the majority of patients, is evident with type-2 *NF1* deletions. This notwithstanding, the breakpoints of type-2 *NF1* deletions are not randomly distributed. Indeed, we noted a disproportionate number of short sequences within the recombination regions (RRs) that are capable of forming non-B DNA. These repeats may well have contributed to the formation of DSBs (Wells, 2007) that then triggered the NAHR events which ultimately gave rise to the type-2 *NF1* deletions. There may also have been some synergy between these repeats and the *Alu* elements noted at the breakpoints of 10 of the 16 intrachromosomal NAHR-mediated type-2 deletions. *Alu* elements are well known recombinogenic sequences [Witherspoon et al., 2009; Konkel and Batzer, 2010] and hence probably also contributed to local DSB formation and subsequent NAHR underlying the type-2 deletions.

A degenerate 13 bp sequence motif has recently been found to be enriched within recombination hotspots [Myers et al., 2008]. Although this motif is present within the PRS2 hotspot in the NF1-REPs, it was absent from the breakpoint regions of the type-2 *NF1* deletions (Supp. Table S8). However, while primary sequence determinants appear to be necessary, they are insufficient to activate recombination [Arnheim et al., 2007; Jeffreys and Neumann, 2009; Myers et al., 2010]. Thus, in addition to the presence of specific sequence motifs, other factors such as histone modification [Buard et al., 2009], the binding of specific proteins e.g. Prdm9 [Mets and Myers, 2009; Parvanov et al., 2009; Baudat et al., 2010] and chromatin structure [Berchowitz et al., 2009] are likely to influence both the location and activity of meiotic recombination hotspots [Székvölgyi and Nicolas, 2009; Paigen and Petkov, 2010]. We have noted marked differences between type-1 and type-2 *NF1* deletion breakpoints in terms of their physical properties. Thus, both GC-content and DNA duplex stability were considerably higher within the meiotic PRS1 and PRS2 NAHR hotspots causing type-1 *NF1* deletions than within the mitotic type-2 *NF1* deletion breakpoints (Supp. Tables S10, S11). Hence, we conclude that in addition to differences in chromosomal origin,

Deleted: of type-2 deletions

Deleted: , CCNCCNTNNCCNC,

Deleted: both allelic and non-allelic homologous

Deleted: clearly

For Peer Review

there are probably substantial differences between mitotic and meiotic NAHR events in the *NF1* gene region with respect to the presence or absence of recombination hotspots as well as GC-content and DNA stability in the respective breakpoint regions. Perhaps significantly, Spo11, which binds to DSBs and initiates meiotic NAHR, is not expressed in mammalian mitotic cells [Shannon et al., 1999; Nogués et al., 2009]. It remains to be seen whether these differences between meiotic and mitotic NAHR are specific to the *NF1* gene region or whether they may instead reflect a more general difference in the mechanism(s) underlying germline and somatic gross chromosomal rearrangements.

Acknowledgement

This work was supported by grants from the DFG [KE 724/7-1; KE 724/9-1 (H.K.S.) and MA 2299/7-1 (V.F.M.)] and from the Deutsche Krebshilfe (#108793, H.K.S., V.F.M.).

For Peer Review

References:

Abeysinghe SS, Chuzhanova N, Krawczak M, Ball EV, Cooper DN. 2003. Translocation and gross deletion breakpoints in human inherited disease and cancer I: Nucleotide composition and recombination-associated motifs. Hum Mutat 22:229-244.

Adler ID. 1996. Comparison of the duration of spermatogenesis between male rodents and humans. Mutat Res 352:169-172.

Arnheim N, Calabrese P, Tiemann-Boege I. 2007. Mammalian meiotic recombination hot spots. Annu Rev Genet 41:369-399.

Ball EV, Stenson PD, Abeysinghe SS, Krawczak M, Cooper DN, Chuzhanova NA. 2005. Microdeletions and microinsertions causing human genetic disease: common mechanisms of mutagenesis and the role of local DNA sequence complexity. Hum Mutat 26:205-213.

Baudat F, Buard J, Grey C, Fledel-Alon A, Ober C, Przeworski M, Coop G, de Massy B. 2010. *PRDM9* is a major determinant of meiotic recombination hotspots in humans and mice. Science 327:836-840.

Bauters M, Van Esch H, Friez MJ, Boespflug-Tanguy O, Zenker M, Vianna-Morgante AM, Rosenberg C, Ignatius J, Raynaud M, Hollanders K, Govaerts K, Vandenreijt K, Niel F, Blanc P, Stevenson RE, Fryns JP, Marynen P, Schwartz CE, Froyen G. 2008. Nonrecurrent *MECP2* duplications mediated by genomic architecture-driven DNA breaks and break-induced replication repair. Genome Res 18:847-858.

For Peer Review

Berchowitz LE, Hanlon SE, Lieb JD, Copenhaver GP. 2009. A positive but complex association between meiotic double-strand break hotspots and open chromatin in *Saccharomyces cerevisiae*. Genome Res 19:2245-2257.

Breslauer KJ, Frank R, Blöcker H, Marky LA. 1986. Predicting DNA duplex stability from the base sequence. Proc Natl Acad Sci USA 83:3746-3750.

Buard J, Barthès P, Grey C, de Massy B. 2009. Distinct histone modifications define initiation and repair of meiotic recombination in the mouse. EMBO J 28:2616-2624.

Bzymek M, Thayer NH, Oh SD, Kleckner N, Hunter N. 2010. Double Holliday junctions are intermediates of DNA break repair. Nature 464:937-941.

Carvalho CM, Zhang F, Lupski JR. 2010. Evolution in Health and Medicine Sackler Colloquium: Genomic disorders: a window into human gene and genome evolution. Proc Natl Acad Sci USA 107 Suppl 1:1765-1771.

Chuzhanova N, Chen JM, Bacolla A, Patrinos GP, Férec C, Wells RD, Cooper DN. 2009. Gene conversion causing human inherited disease: evidence for involvement of non-B-DNA-forming sequences and recombination-promoting motifs in DNA breakage and repair. Hum Mutat 30:1189-1198.

Cullen M, Perfetto SP, Klitz W, Nelson G, Carrington M. 2002. High-resolution patterns of meiotic recombination across the human major histocompatibility complex. Am J Hum Genet 71:759-776.

For Peer Review

De Raedt T, Stephens M, Heyns I, Brems H, Thijs D, Messiaen L, Stephens K, Lazaro C, Wimmer K, Kehrer-Sawatzki H, Vidaud D, Kluwe L, Marynen P, Legius E. 2006. Conservation of hotspots for recombination in low-copy repeats associated with the NF1 microdeletion. Nat Genet 38:1419-1423.

Ding DQ, Haraguchi T, Hiraoka Y. 2010. From meiosis to postmeiotic events: alignment and recognition of homologous chromosomes in meiosis. FEBS J 277:565-570.

Dorschner MO, Sybert VP, Weaver M, Pletcher BA, Stephens K. 2000. *NF1* microdeletion breakpoints are clustered at flanking repetitive sequences. Hum Mol Genet 9:35-46.

Forbes SH, Dorschner MO, Le R, Stephens K. 2004. Genomic context of paralogous recombination hotspots mediating recurrent NF1 region microdeletion. Genes Chrom Cancer 41:12-25.

Garcia-Linares C, Fernández-Rodríguez J, Terribas E, Mercadé J, Pros E, Benito L, Benavente Y, Capella G, Ravella A, Blanco I, Kehrer-Sawatzki H, Lázaro C, Serra E. 2010. Dissecting loss of heterozygosity (LOH) in neurofibromatosis type 1-associated neurofibromas: importance of copy neutral LOH. Hum Mutat, in press

Gerton JL, Hawley RS. 2005. Homologous chromosome interactions in meiosis: diversity amidst conservation. Nat Rev Genet 6:477-487.

Gu W, Zhang F, Lupski JR. 2008. Mechanisms for human genomic rearrangements. Pathogenetics 1:4.

For Peer Review

Gusev VD, Nemytikova LA, Chuzhanova NA. 1999. On the complexity measures of genetic sequences. Bioinformatics 15:994-999.

Hagstrom SA, Dryja TP. 1999. Mitotic recombination map of 13cen-13q14 derived from an investigation of loss of heterozygosity in retinoblastomas. Proc Natl Acad Sci USA 96:2952-2957.

Hastings PJ, Ira G, Lupski JR. 2009. A microhomology-mediated break-induced replication model for the origin of human copy number variation. PLoS Genet 5:e1000327.

Howarth K, Ranta S, Winter E, Teixeira A, Schaschl H, Harvey JJ, Rowan A, Jones A, Spain S, Clark S, Guenther T, Stewart A, Silver A, Tomlinson I. 2009. A mitotic recombination map proximal to the *APC* locus on chromosome 5q and assessment of influences on colorectal cancer risk. BMC Med Genet 10:54.

Hurles ME, Lupski JR. 2006. Recombination hotspots in nonallelic homologous recombination. In: Lupski JR, Stankiewicz P (eds) Genomic disorders: the genomic basis of disease. Humana Press, Totawa, New Jersey

Jeffreys AJ, Neumann R. 2009. The rise and fall of a human recombination hot spot. Nat Genet 41:625-629.

Jenne DE, Tinschert S, Reimann H, Lasinger W, Thiel G, Hameister H, Kehrer-Sawatzki H. 2001. Molecular characterization and gene content of breakpoint boundaries in patients with neurofibromatosis type 1 with 17q11.2 microdeletions. Am J Hum Genet 69:516-527.

For Peer Review

Jenne DE, Tinschert S, Dorschner MO, Hameister H, Stephens K, Kehrer-Sawatzki H. 2003. Complete physical map and gene content of the human *NF1* tumor suppressor region in human and mouse. Genes Chrom Cancer 37:111-120.

Kauppi L, Jeffreys AJ, Keeney S. 2004. Where the crossovers are: recombination distributions in mammals. Nat Rev Genet 5:413-424.

Kehrer-Sawatzki H, Kluwe L, Sandig C, Kohn M, Wimmer K, Krammer U, Peyrl A, Jenne DE, Hansmann I, Mautner VF. 2004. High frequency of mosaicism among patients with neurofibromatosis type 1 (NF1) with microdeletions caused by somatic recombination of the *JJAZ1* gene. Am J Hum Genet 75:410-423.

Konkel MK, Batzer MA. 2010. A mobile threat to genome stability: The impact of non-LTR retrotransposons upon the human genome. Semin Cancer Biol Mar 20 [Epub ahead of print]

Krogh BO, Symington LS. 2004. Recombination proteins in yeast. Annu Rev Genet 38:233-271.

Kurotaki N, Stankiewicz P, Wakui K, Niikawa N, Lupski JR. 2005. Sotos syndrome common deletion is mediated by directly oriented subunits within inverted SoS-REP low-copy repeats. Hum Mol Genet 14:535–542.

LaFave MC, Sekelsky J. 2009. Mitotic recombination: why? when? how? where? PLoS Genet 5:e1000411.

For Peer Review

Lam KW, Jeffreys AJ. 2007. Processes of *de novo* duplication of human alpha-globin genes. Proc Natl Acad Sci USA 104:10950-10955.

Lam HY, Mu XJ, Stütz AM, Tanzer A, Cayting PD, Snyder M, Kim PM, Korbel JO, Gerstein MB. 2010. Nucleotide-resolution analysis of structural variants using BreakSeq and a breakpoint library. Nat Biotechnol 28:47-55.

Lee JA, Carvalho C, Lupski JR. 2007. A DNA replication mechanism for generating nonrecurrent rearrangements associated with genomic disorders. Cell 131:1235–1247.

Lieber MR. 2010. The mechanism of double-dtrand DNA break repair by the nonhomologous DNA end-joining pathway. Annu Rev Biochem 79:1.1–1.31.

Lindsay SJ, Khajavi M, Lupski JR, Hurles ME. 2006. A chromosomal rearrangement hotspot can be identified from population genetic variation and is coincident with a hotspot for allelic recombination. Am J Hum Genet 79:890-902.

López-Correa C, Brems H, Lázaro C, Marynen P, Legius E. 2000. Unequal meiotic crossover: a frequent cause of NF1 microdeletions. Am J Hum Genet 66:1969-1974.

López-Correa C, Dorschner M, Brems H, Lázaro C, Clementi M, Upadhyaya M, Dooijes D, Moog U, Kehrer-Sawatzki H, Rutkowski JL, Fryns JP, Marynen P, Stephens K, Legius E. 2001. Recombination hotspot in NF1 microdeletion patients. Hum Mol Genet 10:1387-1392.

Deleted: Loidl J. 2006. *S. pombe* linear elements: the modest cousins of synaptonemal complexes. Chromosoma 115:260-271. ¶

For Peer Review

Lupski JR. 2004. Hotspots of homologous recombination in the human genome: not all homologous sequences are equal. Genome Biol 5:242.

Lupski JR, Stankiewicz P. 2005. Genomic disorders: molecular mechanisms for rearrangements and conveyed phenotypes. PLoS Genet 1:e49.

Lupski JR. 2009. Genomic disorders ten years on. Genome Med 1:42.

Makridakis NM, Caldas Ferraz LF, Reichardt JK. 2009. Genomic analysis of cancer tissue reveals that somatic mutations commonly occur in a specific motif. Hum Mutat 30:39-48.

Mao Z, Bozzella M, Seluanov A, Gorbunova V. 2008. DNA repair by nonhomologous end joining and homologous recombination during cell cycle in human cells. Cell Cycle 7:2902-2906.

Meaburn KJ, Misteli T. 2007. Cell biology: chromosome territories. Nature 445:379-781.

Mefford HC, Eichler EE. 2009. Duplication hotspots, rare genomic disorders, and common disease. Curr Opin Genet Dev 19:196-204.

Mets DG, Meyer BJ. 2009. Condensins regulate meiotic DNA break distribution, thus crossover frequency, by controlling chromosome structure. Cell 139:73-86.

Moynahan ME, Jasin M. 2010. Mitotic homologous recombination maintains genomic stability and suppresses tumorigenesis. Nat Rev Mol Cell Biol 11:196-207.

For Peer Review

Myers S, Bottolo L, Freeman C, McVean G, Donnelly P. 2005. A fine-scale map of recombination rates and hotspots across the human genome. Science 310:321–324.

Myers S, Freeman C, Auton A, Donnelly P, McVean G. 2008. A common sequence motif associated with recombination hot spots and genome instability in humans. Nat Genet 40:1124-1129.

Myers S, Bowden R, Tumian A, Bontrop RE, Freeman C, Macfie TS, McVean G, Donnelly P. 2010. Drive against hotspot motifs in primates implicates the *PRDM9* gene in meiotic recombination. Science 327:876-879.

Nogués C, Fernández C, Rajmil O, Templado C. 2009. Baseline expression profile of meiotic-specific genes in healthy fertile males. Fertil Steril 92:578-582.

Paigen K, Petkov P. 2010. Mammalian recombination hot spots: properties, control and evolution. Nat Rev Genet 11:221-233.

Parvanov ED, Petkov PM, Paigen K. 2009. *Prdm9* controls activation of mammalian recombination hotspots. Science 327:835.

Petek E, Jenne DE, Smolle J, Binder B, Lasinger W, Windpassinger C, Wagner K, Kroisel PM, Kehrer-Sawatzki H. 2003. Mitotic recombination mediated by the *JJAZF1* (KIAA0160) gene causing somatic mosaicism and a new type of constitutional NF1 microdeletion in two children of a mosaic female with only few manifestations. J Med Genet 40:520-525.

For Peer Review

Reiter LT, Hastings PJ, Nelis E, De Jonghe P, Van Broeckhoven C, Lupski JR. 1998. Human meiotic recombination products revealed by sequencing a hotspot for homologous strand exchange in multiple HNPP deletion patients. Am J Hum Genet 62:1023-1033.

Rockmill B, Roeder GS. 1990. Meiosis in asynaptic yeast. Genetics 126:563-574.

Roeder GS. 1997. Meiotic chromosomes: it takes two to tango. Genes Dev 11:2600-2621.

Roehl AC, Cooper DN, Kluwe L, Helbrich A, Wimmer K, Högel J, Mautner VF, Kehrer-Sawatzki H. 2010. Extended runs of homozygosity at 17q11.2: an association with type-2 NF1 deletions? Hum Mutat 31:325-334.

Sasaki M, Lange J, Keeney S. 2010. Genome destabilization by homologous recombination in the germ line. Nat Rev Mol Cell Biol 11:182-195.

Serra E, Rosenbaum T, Nadal M, Winner U, Ars E, Estivill X, Lázaro C. 2001. Mitotic recombination effects homozygosity for *NF1* germline mutations in neurofibromas. Nat Genet 28:294-296.

Shannon M, Richardson L, Christian A, Handel MA, Thelen MP. 1999. Differential gene expression of mammalian *SPO11/TOP6A* homologs during meiosis. FEBS Lett 462:329-334.

Shaw CJ, Withers MA, Lupski JR. 2004. Uncommon deletions of the Smith-Magenis syndrome region can be recurrent when alternate low-copy repeats act as homologous recombination substrates. Am J Hum Genet 75:75-81.

For Peer Review

Shaw CJ, Lupski JR. 2004. Implications of human genome architecture for rearrangement-based disorders: the genomic basis of disease. Hum Mol Genet 13:R57-R64.

Sjögren C, Nasmyth K. 2001. Sister chromatid cohesion is required for postreplicative double-strand break repair in *Saccharomyces cerevisiae*. Curr Biol 11:991-995.

Stanfield SW, Helinski DR. 1984. Cloning and characterization of small circular DNA from Chinese hamster ovary cells. Mol Cell Biol 4:173-180.

Stankiewicz P, Lupski JR. 2010. Structural variation in the human genome and its role in disease. Annu Rev Med 61:437-455.

Steele DF, Morris ME, Jinks-Robertson S. 1991. Allelic and ectopic interactions in recombination-defective yeast strains. Genetics 127:53-60

Steinmann K, Cooper DN, Kluwe L, Chuzhanova NA, Senger C, Serra E, Lázaro C, Gilaberte M, Wimmer K, Mautner VF, Kehrer-Sawatzki H. 2007. Type 2 *NF1* deletions are highly unusual by virtue of the absence of nonallelic homologous recombination hotspots and an apparent preference for female mitotic recombination. Am J Hum Genet 81:1201-1220.

Steinmann K, Kluwe L, Cooper DN, Brems H, De Raedt T, Legius E, Mautner VF, Kehrer-Sawatzki H. 2008. Copy number variations in the *NF1* gene region are infrequent and do not predispose to recurrent type-1 deletions. Eur J Hum Genet 16:572-580.

For Peer Review

Steinmann K, Kluwe L, Friedrich RE, Mautner VF, Cooper DN, Kehrer-Sawatzki H. 2009. Mechanisms of loss of heterozygosity in neurofibromatosis type 1-associated plexiform neurofibromas. J Invest Dermatol 129:615-621.

Stephens K, Weaver M, Leppig KA, Maruyama K, Emanuel PD, Le Beau MM, Shannon KM. 2006. Interstitial uniparental isodisomy at clustered breakpoint intervals is a frequent mechanism of NF1 inactivation in myeloid malignancies. Blood 108:1684-1689.

Székvölgyi L, Nicolas A. 2009. From meiosis to postmeiotic events: homologous recombination is obligatory but flexible. FEBS J 277:571-589.

Thomas NS, Durkie M, Potts G, Sandford R, Van Zyl B, Youings S, Dennis NR, Jacobs PA. 2006. Parental and chromosomal origins of microdeletion and duplication syndromes involving 7q11.23, 15q11-q13 and 22q11. Eur J Hum Genet 14:831-837.

Torres-Juan L, Rosell J, Sánchez-de-la-Torre M, Fibla J, Heine-Suñer D. 2007. Analysis of meiotic recombination in 22q11.2, a region that frequently undergoes deletions and duplications. BMC Med Genet 8:14.

Turner DJ, Miretti M, Rajan D, Fiegler H, Carter NP, Blayney ML, Beck S, Hurles ME. 2008. Germline rates of *de novo* meiotic deletions and duplications causing several genomic disorders. Nat Genet 40:90-95.

Upadhyaya M, Ruggieri M, Maynard J, Osborn M, Hartog C, Mudd S, Penttinen M, Cordeiro I, Ponder M, Ponder BA, Krawczak M, Cooper DN. 1998. Gross deletions of the neurofibromatosis type 1 (*NF1*) gene are predominantly of maternal origin and commonly

Deleted: Storlazzi A, Xu L, Schwacha A, Kleckner N. 1996. Synaptonemal complex (SC) component *Zip1* plays a role in meiotic recombination independent of SC polymerization along the chromosomes. Proc Natl Acad Sci USA 93:9043-9048.¶
¶
Sym M, Roeder GS. 1994. Crossover interference is abolished in the absence of a synaptonemal complex protein. Cell 79:283-292.¶
¶

For Peer Review

associated with a learning disability, dysmorphic features and developmental delay. Hum Genet 102:591-597.

Upadhyaya M, Spurlock G, Kluwe L, Chuzhanova N, Bennett E, Thomas N, Guha A, Mautner V. 2009. The spectrum of somatic and germline *NF1* mutations in NF1 patients with spinal neurofibromas. Neurogenetics 10:251-263.

Visser R, Shimokawa O, Harada N, Kinoshita A, Ohta T, Niikawa N, Matsumoto N. 2005. Identification of a 3.0-kb major recombination hotspot in patients with Sotos syndrome who carry a common 1.9-Mb microdeletion. Am J Hum Genet 76:52-67.

Vissers LE, Bhatt SS, Janssen IM, Xia Z, Lalani SR, Pfundt R, Derwinska K, de Vries BB, Gilissen C, Hoischen A, Nesteruk M, Wisniowiecka-Kowalnik B, Smyk M, Brunner HG, Cheung SW, van Kessel AG, Veltman JA, Stankiewicz P. 2009. Rare pathogenic microdeletions and tandem duplications are microhomology-mediated and stimulated by local genomic architecture. Hum Mol Genet 18:3579-3593.

Wells RD. 2007. Non-B DNA conformations, mutagenesis and disease. Trends Biochem Sci 32:271-278.

Witherspoon DJ, Watkins WS, Zhang Y, Xing J, Tolpinrud WL, Hedges DJ, Batzer MA, Jorde LB. 2009. *Alu* repeats increase local recombination rates. BMC Genomics 10:530.

Wu ZK, Getun IV, Bois PR. 2010. Anatomy of mouse recombination hot spots. Nucleic Acids Res 38:2346-2354.

For Peer Review

Xu L, Weiner BM, Kleckner N. 1997. Meiotic cells monitor the status of the interhomolog recombination complex. Genes Dev 11:106-118.

Zeitz MJ, Mukherjee L, Bhattacharya S, Xu J, Berezney R. 2009. A probabilistic model for the arrangement of a subset of human chromosome territories in WI38 human fibroblasts. J Cell Physiol 221:120-129.

Zhang F, Gu W, Hurles ME, Lupski JR. 2009a. Copy number variation in human health, disease, and evolution. Annu Rev Genomics Hum Genet 10:451-481.

Zhang F, Khajavi M, Connolly AM, Towne CF, Batish SD, Lupski JR. 2009b. The DNA replication FoSTeS/MMBIR mechanism can generate genomic, genic and exonic complex rearrangements in humans. Nat Genet 41:849-853.

Zhang F, Carvalho CM, Lupski JR. 2009c. Complex human chromosomal and genomic rearrangements. Trends Genet 25:298-307.

Zhang F, Potocki L, Sampson JB, Liu P, Sanchez-Valle A, Robbins-Furman P, Navarro AD, Wheeler PG, Spence JE, Brasington CK, Withers MA, Lupski JR. 2010. Identification of uncommon recurrent Potocki-Lupski syndrome-associated duplications and the distribution of rearrangement types and mechanisms in PTLS. Am J Hum Genet 86:462-470.

For Peer Review

Legends to Figures

Figure 1: Map of the *NF1* gene region at 17q11.2 showing the positions of the breakpoints identified in the 18 patients with type-2 *NF1* deletions. (A) The relative positions of the *NF1* gene, the *SUZ12* gene and its pseudogene (*SUZ12P*) are specifically indicated. The other genes located in this region are represented by black bars. (B) The positions of the type-2 deletion breakpoints arising from NAHR identified in most patients (indicated by vertical red lines) were located at homologous sites within *SUZ12* and *SUZ12P*. By contrast, the type-2 deletion breakpoints in patients HC and 928 (indicated by vertical blue lines) were not located at homologous sites within *SUZ12* and *SUZ12P*. The exons within the *SUZ12* and *SUZ12P* sequences are denoted by numbered vertical bars. The circles represent the juxtaposed breakpoints of patients WB and UC172 which occurred within identical 174 bp intervals.

Figure 2: Intrachromosomal NAHR between the *SUZ12* gene (red rectangle) and the highly homologous *SUZ12P* sequence (blue rectangle) is accompanied by the maintenance of heterozygosity distal to the rearrangements. (A) If intrachromosomal NAHR occurs during G1-phase, this yields, after replication and mitosis, cells bearing the deletion on one chromosome. The reciprocal acentric fragment is lost during subsequent cell divisions. Type-2 *NF1* deletions occur during the embryonic development of affected patients and hence, in addition to cells harbouring the deletion, normal cells lacking the deletion are invariably also present in the soma of the respective patients (not shown in this schema). (B) If intrachromosomal NAHR occurs post-replication, this could either be within one chromatid or between sister-chromatids. Only NAHR between sister-chromatids yields cells with the reciprocal duplication.

For Peer Review

Figure 3: Interchromosomal NAHR between the *SUZ12* gene (red rectangle) and the highly homologous *SUZ12P* sequence (blue rectangle) giving rise to type-2 *NF1* deletions. (A) Interchromatid NAHR in G1-phase would not result in a detectable copy number change since the deletions and their reciprocal duplications would be present in the same cells. (B) Interchromosomal NAHR between non-sister chromatids would either not result in a detectable copy number change or would lead to loss of heterozygosity (homozygosity) distal to the deletion depending upon the segregation of the chromatids after the subsequent mitosis.

Figure 4: Map of the *NF1* gene region (and the genes located therein) in relation to the relative positions of runs of homozygosity (ROHs; indicated as blue bars) in a size range of 202 kb to 568 kb immediately flanking the type-2 *NF1* deletions in a telomeric direction. Such ROHs were noted in 13 patients. The type-2 *NF1* deletions are depicted as grey bars.

For Peer Review

Table 1: Localization and extent of the type-2 deletion breakpoint regions (recombination regions) identified in 18 NF1 patients

Patient	Deletion breakpoint regions in *SUZ12P*	Deletion breakpoint regions in *SUZ12*	Length of the recombination region (bp)	Breakpoint localization within *SUZ12P/SUZ12*
811-M[a]	26,093,151-26,093,196	27,297,456-27,297,501	46	Intron 3
KCD[b]	26,095,311-26,095,419	27,299,613-27,299,721	109	Intron 4
697[a]	26,100,313-26,100,381	27,304,631-27,304,699	69	Intron 4
736[a]	26,104,591-26,104,678	27,308,895-27,308,982	88	Intron 4
1630[a]	26,108,823-26,108,934	27,313,160-27,313,271	112	Intron 4
2358[c]	26,109,915-26,109,978	27,316,556-27,316,619	64	Intron 4
585[c]	26,109,980-26,110,109	27,316,621-27,316,750	130	Intron 4
488[a]	26,111,549-26,111,605	27,318,189-27,318,245	57	Intron 5
1502[a]	26,111,715-26,111,905	27,318,355-27,318,545	191	Intron 5
1956[c]	26,112,365-26,112,510	27,318,916-27,319,061	146	Intron 5
IL39[b]	26,115,506-26,115,552	27,322,062-27,322,108	47	Intron 5
1104[a]	26,115,602-26,115,677	27,322,154-27,322,229	76	Intron 5
928[a]	26,117,984	27,327,893	—	Intron 6/Intron 8
2429[c]	26,122,947-26,123,171	27,329,593-27,329,817	225	Intron 8
WB[b]	26,125,230-26,125,406	27,331,894-27,332,070	177	Intron 8
UC172[c]	26,125,230-26,125,406	27,331,894-27,332,070	177	Intron 8
938[a]	26,127,646-26,127,756	27,334,336-27,334,446	111	Exon 9
HC[a]	26,104,116	27,339,771	—	Intron 4/Intron 10

[a] as determined in Steinmann et al. [2007]
[b] as determined in Kehrer-Sawatzki et al. [2004]
[c] as determined in this study
—: the deletion was not caused by NAHR and hence recombination regions were not observed. Since the breakpoints of the deletions were located in regions that are not homologous between *SUZ12* and *SUZ12P*, the breakpoints could be determined precisely. Nucleotide numbering is according to hg18, NCBI 36.

For Review

Table 2: Mechanisms underlying the 18 type-2 *NF1* deletions and parental origin of the chromosomes 17 harbouring the deletions

Patient	Type of recombination causing the deletions	Mechanism as determined by SNP arrays	Mechanism as determined by microsatellite marker analysis[b]	Parental origin of the chromosome 17 harbouring the type 2 *NF1* deletion
811-M	NAHR	intrachromosomal	intrachromosomal	paternal
KCD	NAHR	intrachromosomal	intrachromosomal	n.d.
697	NAHR	intrachromosomal	intrachromosomal	maternal
736	NAHR	intrachromosomal	intrachromosomal	n.d.
1630	NAHR	intrachromosomal	intrachromosomal	paternal
2358	NAHR	n.d.	intrachromosomal	maternal
585	NAHR	intrachromosomal	intrachromosomal	maternal
488	NAHR	intrachromosomal	intrachromosomal	paternal
1502	NAHR	intrachromosomal	intrachromosomal	maternal
1956	NAHR	intrachromosomal	intrachromosomal	n.d.
IL39	NAHR	intrachromosomal	intrachromosomal	maternal
1104	NAHR	intrachromosomal	intrachromosomal	n.d.
928[a]	NHEJ	intrachromosomal	intrachromosomal	maternal
2429	NAHR	n.d.	interchromosomal	paternal
WB	NAHR	intrachromosomal	intrachromosomal	n.d.
938	NAHR	intrachromosomal	intrachromosomal	maternal
HC[a]	NHEJ	n.d.	intrachromosomal	maternal
UC172	NAHR	intrachromosomal	intrachromosomal	maternal

n.d.: not determined

a: The deletions of patients 928 and HC have breakpoints in apparently non-homologous regions between *SUZ12* and *SUZ12P*.

NHEJ: non-homologous end joining; NAHR: non-allelic homologous recombination

For Peer Review

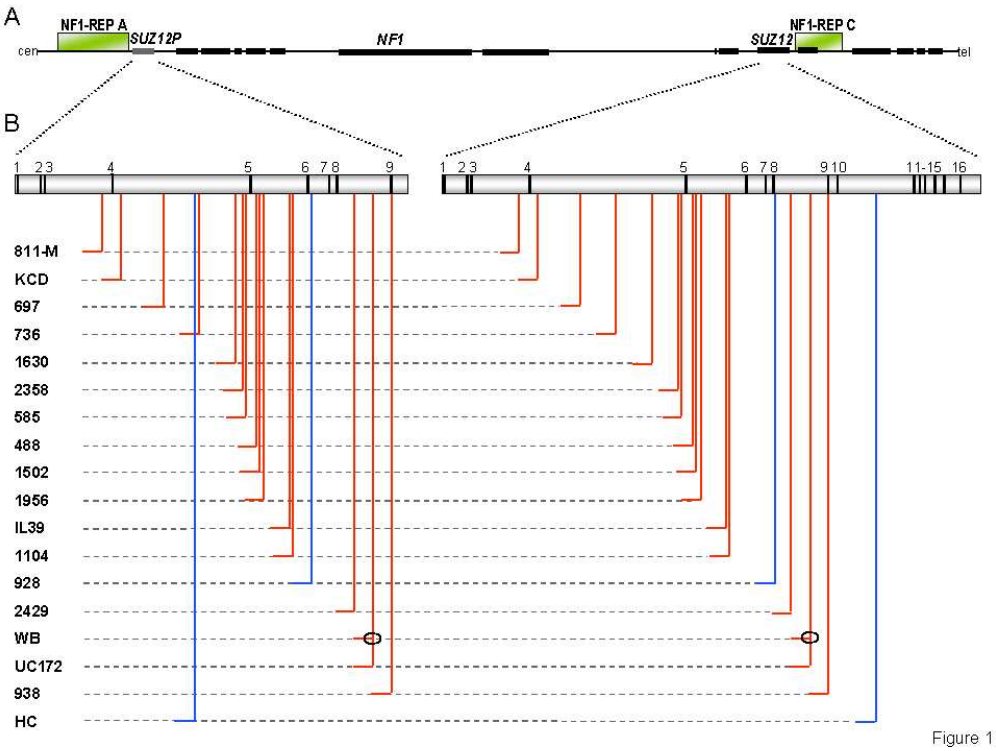

Figure 1

81x60mm (300 x 300 DPI)

Review

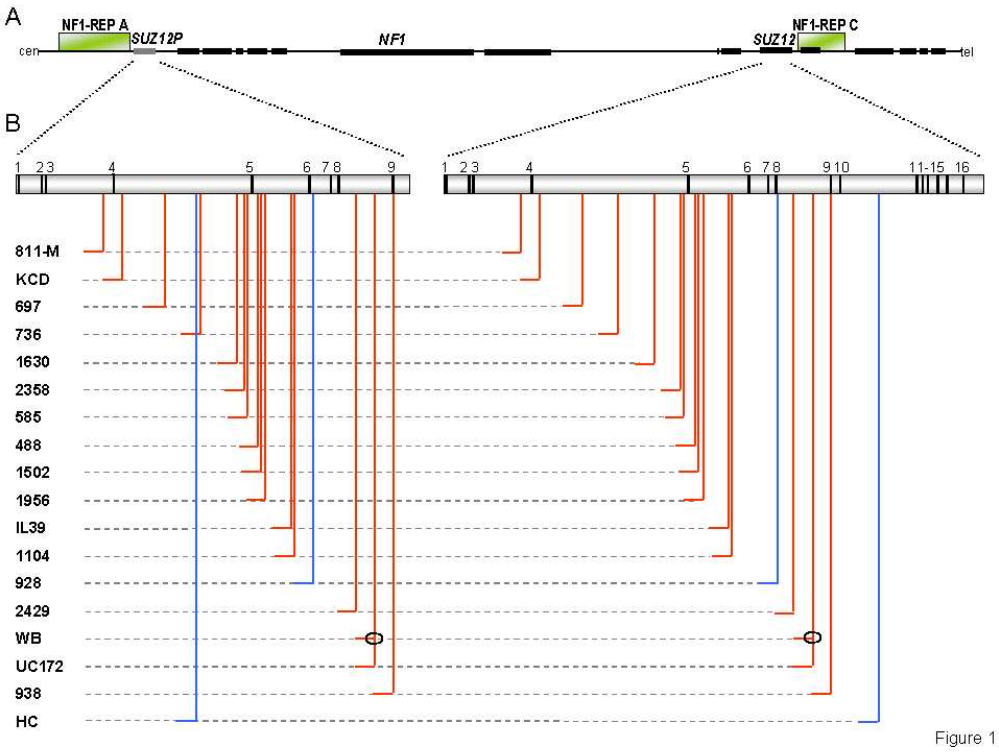

Figure 1

81x60mm (300 x 300 DPI)

Review

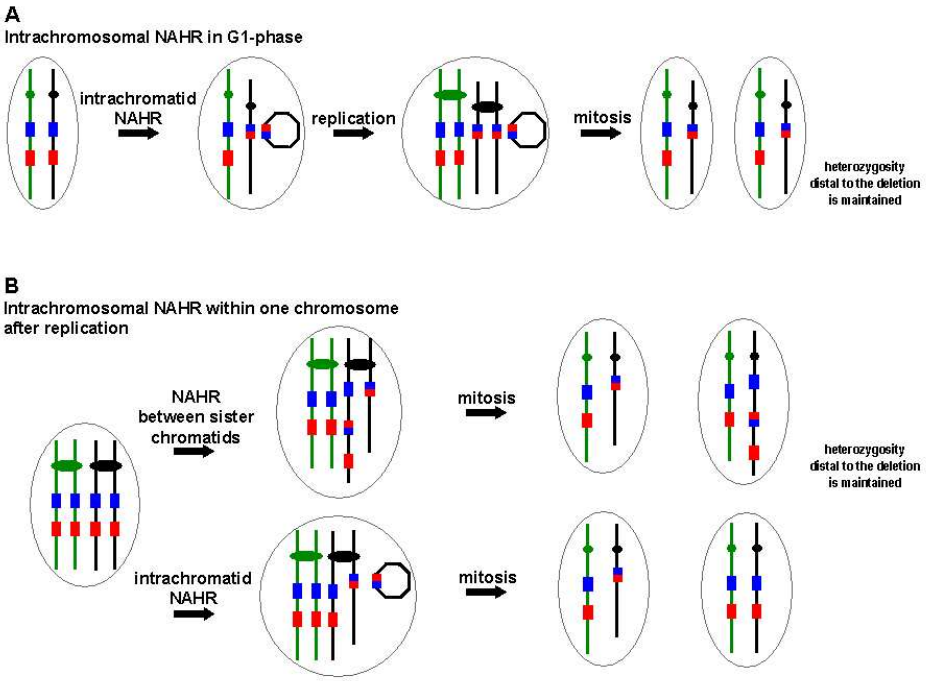

Figure 2

81x60mm (300 x 300 DPI)

Review

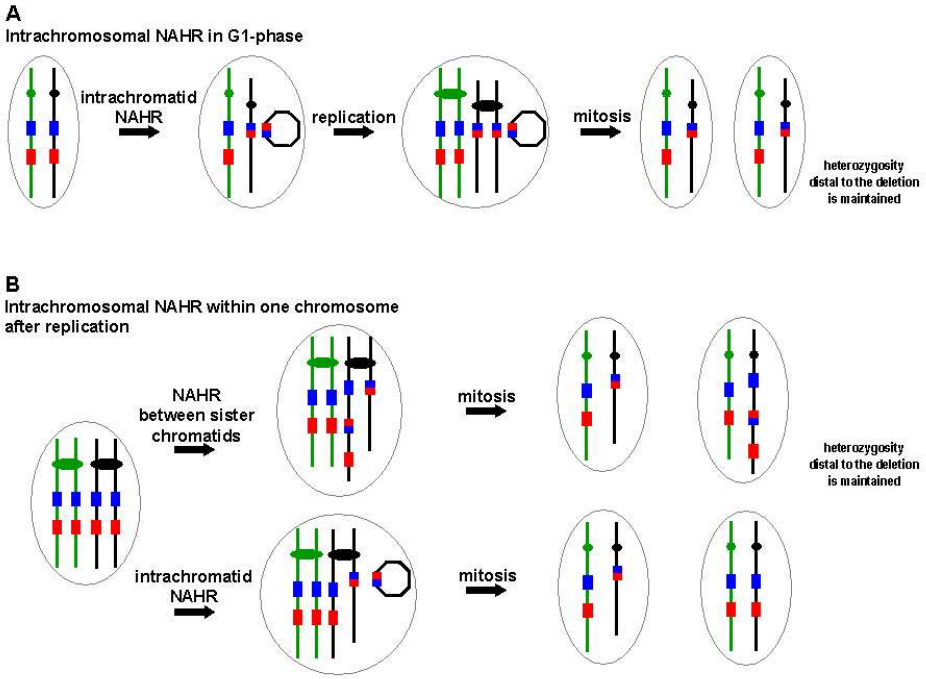

Figure 2

81x60mm (300 x 300 DPI)

eview

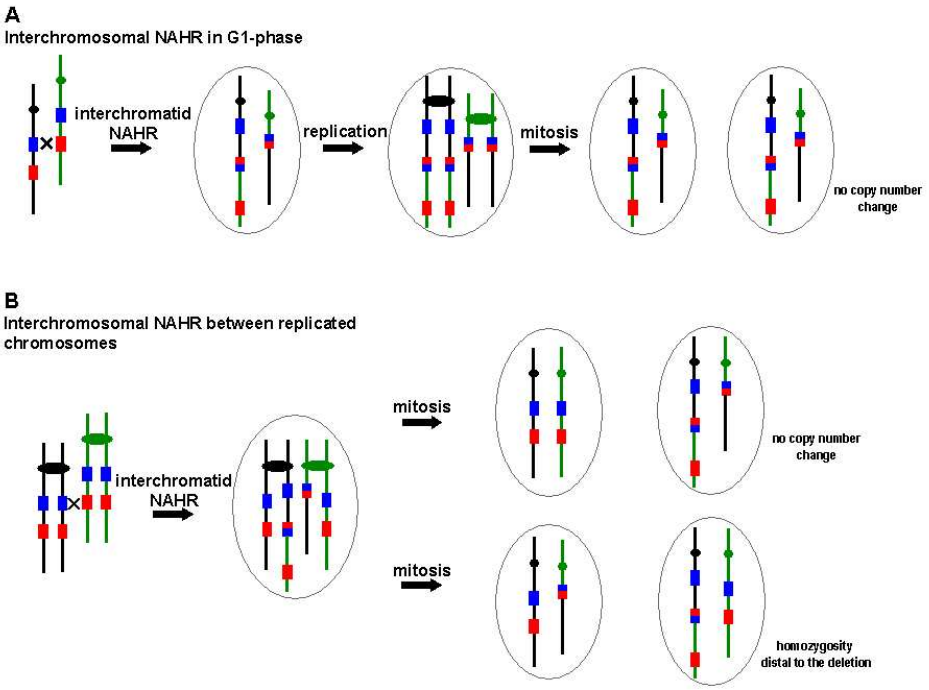

Figure 3

81x60mm (300 x 300 DPI)

Review

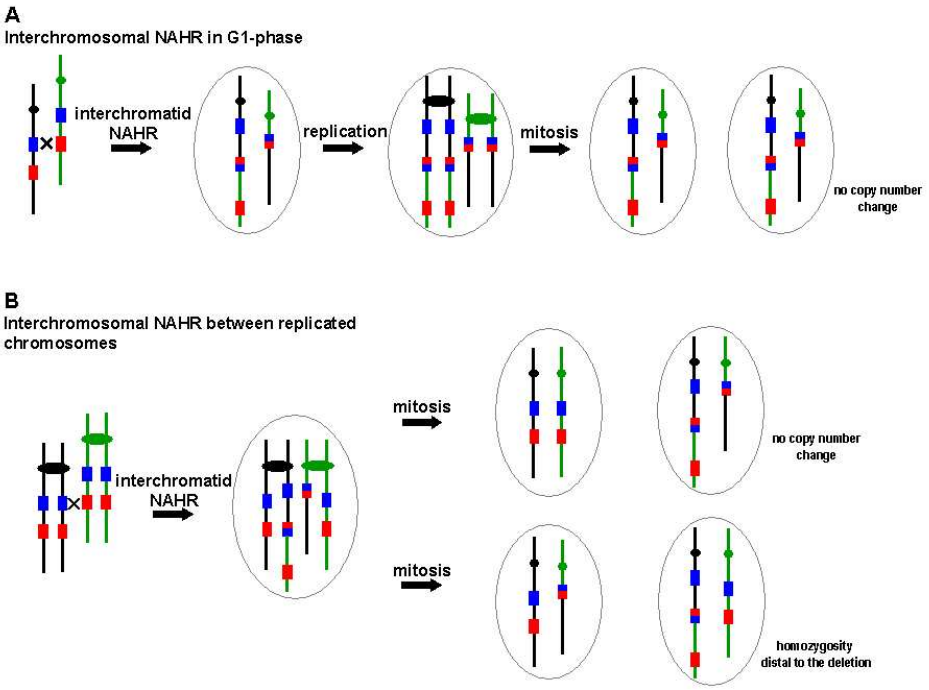

Figure 3

81x60mm (300 x 300 DPI)

Review

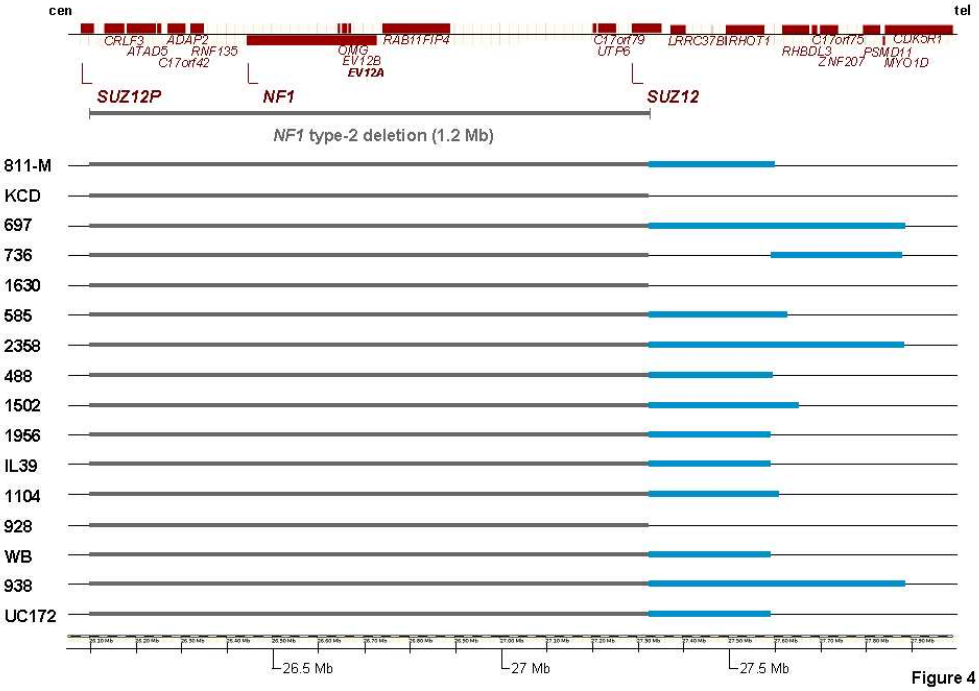

Figure 4

81x60mm (300 x 300 DPI)

Review

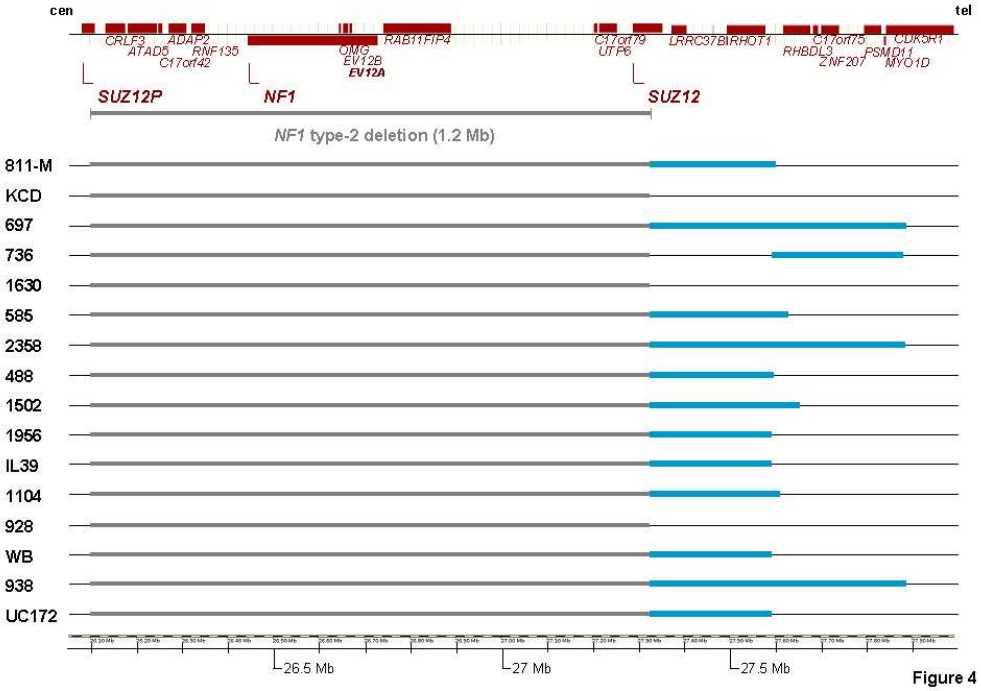

Figure 4

81x60mm (300 x 300 DPI)

Position of marker on chromosome 17	Marker	Patient 811-1 Blood		Mother (811-M) of patient 811-1 Blood		Grandmother of patient 811-1 Blood		Grandfather of patient 811-1 Blood	
24,481,596 – 24,481,738	D17S1873	146	130	124	130	124	138	120	130
24,885,942 – 24,886,214	D17S1841	274	272	272	272	272	270	264	272
25,124,113 – 25,124,371	D17S975	254	254	258	254	258	258	254	254
25,708,122 – 25,708,291	D17S1532	170	170	172	170	172	170	170	170
26,614,048 – 26,614,348	NF1PCR3	266	del	266	--	266	272	262	266
26,650,321 – 26,650,578	D17S2162	257	del	257	--	257	257	261	257
26,664,798 – 26,665,027	IVs27TG24.8	272	del	280	--	280	272	274	280
26,668,420 – 26,668,626	IVs27AC28.4	207	del	205	--*	205	207	215	207
26,673,142 – 26,673,342	D17S1166	194	del	202	(194)	202	194	202	194
26,960,942 – 26,961,211	D17S1800	276	del	278	(274)	278	272	280	274
28,038,006 – 28,038,197	D17S1880	190	182	190	182	190	190	184	182
29,161,843 – 29,162,110	D17S1850	270	270	266	270	266	264	270	270
30,890,423 – 30,890,752	D17S907	286	340	300	340	300	332	286	340
31,148,163 – 31,148,318	D17S1833	154	154	154	154	154	154	158	154
60,127,912 – 60,128,058	D17S1809	141	147	145	147	145	141	149	147

Supplementary Figure S1-A: Analysis of microsatellite markers on chromosome 17 using DNA extracted from blood samples taken from patient 811-1 and his family members. Patient 811-1 has a constitutional type-2 *NF1* deletion. He is the son of patient 811-M (his mother) who is mosaic for the deletion. Some 93% of cells in the blood of patient 811-M were found to exhibit the deletion as determined by FISH [Steinmann et al., 2007]. The horizontal rectangular box includes those markers located within the deletion region. Marker alleles in parentheses displayed reduced signal intensity, indicative of somatic mosaicism involving both normal cells and cells bearing the deletion.

--: reduced signal intensity of markers which would have been indicative of somatic mosaicism but could not be formally assessed as a consequence of homozygosity.

--*: a second allele was not visible, although heterozygosity was inferred from the grandpaternal haplotype.

del: deletion of the allele.

Nucleotide numbering is according to hg18, NCBI 36.

Position of marker on chromosome 17	Marker	Patient KCD Blood		Hybrid #3	Hybrid #25	Hybrid #101
24,481,596 – 24,481,738	D17S1873	140	140	140	140	140
24,885,942 – 24,886,214	D17S1841	272	270	270	270	272
25,124,113 – 25,124,371	D17S975	258	254	254	254	258
26,497,479 – 26,497,687	D17S1307	210	(202)	del	202	210
26,664,798 – 26,665,027	IVs27TG24.8	280	(272)	del	272	280
26,668,420 – 26,668,626	IVs27AC28.4	209	(207)	del	207	209
26,673,142 – 26,673,342	D17S1166	202	(192)	del	192	202
28,038,006 – 28,038,197	D17S1880	183	181	181	181	183
30,890,423 – 30,890,752	D17S907	311	299	299	299	311
31,148,163 – 31,148,318	D17S1833	156	154	154	154	156
33,160,167 – 33,160,320	D17S1788	155	166	166	166	155

Supplementary Figure S1-B: Analysis of microsatellite markers on chromosome 17 using DNA extracted from peripheral blood taken from patient KCD and hybrid cell lines containing only one chromosome 17 from this patient. Hybrid cell line #3 contains the chromosome 17 with the type-2 *NF1* deletion whereas hybrid cell line #25 contains the normal chromosome 17 which was subject to the deletion in a number of cells. Hybrid cell line #101 contains the wild-type chromosome 17 of the patient. All three somatic cell hybrids were obtained by fusion of skin fibroblasts from patient KCD with mouse cell line B82. In skin fibroblasts from patient KCD, 51% of cells carried the deletion whilst 49% of cells were normal. In peripheral blood, the deletion was detected in 92% of cells as determined by FISH [Kehrer-Sawatzki et al., 2004; Steinmann et al., 2007]. Marker alleles in parentheses displayed reduced signal intensity, indicative of somatic mosaicism involving both normal cells and cells bearing the deletion. The horizontal rectangular box includes those markers located within the deletion region. del: deletion of the allele.
Nucleotide numbering is according to hg18, NCBI 36.

Position of marker on chromosome 17	Marker	Patient 697 Blood		Hybrid #16f	Father of patient 697 Blood		Mother of patient 697 Blood		Sister of patient 697 Blood	
24,481,596 – 24,481,738	D17S1873	142	130	130	142	126	130	134	142	130
24,693,853 – 24,694,013	D17S2093	159	159	159	159	159	159	159	159	159
24,885,942 – 24,886,214	D17S1841	270	270	270	270	272	270	278	270	270
25,124,113 – 25,124,371	D17S975	258	258	258	258	254	258	258	258	258
25,708,122 – 25,708,291	D17S1532	169	175	175	169	169	175	169	169	175
26,497,479 – 26,497,687	D17S1307	206	del	del	206	210	206	210	206	206
26,614,048 – 26,614,348	NF1PCR3	266	del	del	266	266	270	266	266	270
26,641,851 – 26,642,254	D17S2237	400	del	del	400	404	400	404	400	400
26,664,798 – 26,665,027	IVs27TG24.8	272	del	del	272	280	272	280	272	272
26,668,420 – 26,668,626	IVs27AC28.4	207	del	del	207	205	207	213	207	207
26,673,142 – 26,673,342	D17S1166	202	del	del	202	198	198	194	202	198
26,960,942 – 26,961,211	D17S1800	278	del	del	278	264	276	276	278	276
28,038,006 – 28,038,197	D17S1880	188	188	188	188	194	188	192	188	188
29,161,843 – 29,162,110	D17S1850	270	266	266	270	264	266	270	270	266
29,584,279 – 29,584,562	D17S1293	280	270	270	280	264	270	260	280	270
30,890,423 – 30,890,752	D17S907	286	286	286	286	326	286	322	286	286
31,148,163 – 31,148,318	D17S1833	156	156	156	156	154	156	154	156	156
40,162,539 – 40,162,644	D17S1861	106	102	102	106	106	102	106	106	102

Supplementary Figure S1-C: Analysis of microsatellite markers on chromosome 17 using DNA extracted from blood samples taken from patient 697 and her family members. Patient 697 has a mosaic type-2 *NF1* deletion; the proportion of cells harbouring the deletion in peripheral blood was 97% and in buccal smears 59% as determined by FISH [Kehrer-Sawatzki et al., 2004; Steinmann et al., 2007]. The horizontal rectangular box includes those markers located within the deletion region. del: deletion of the allele. Nucleotide numbering is according to hg18, NCBI 36.

Position of marker on chromosome 17	Marker	Patient 736 Blood		Hybrid #15	Hybrid #1	Hybrid #26
24,481,596 – 24,481,738	D17S1873	146	140	140	140	146
24,885,942 – 24,886,214	D17S1841	274	272	272	272	274
25,124,113 – 25,124,371	D17S975	258	254	254	254	258
26,497,479 – 26,497,687	D17S1307	210	(204)	204	del	210
26,641,851 – 26,642,254	D17S2237	400	(396)	396	del	400
26,664,798 – 26,665,027	IVs27TG24.8	280	--	280	del	280
26,668,420 – 26,668,626	IVs27AC28.4	205	(207)	207	del	205
26,673,142 – 26,673,342	D17S1166	202	(198)	198	del	202
26,960,942 – 26,961,211	D17S1800	270	(276)	276	del	270
28,038,006 – 28,038,197	D17S1880	192	174	174	174	192
30,890,423 – 30,890,752	D17S907	324	286	286	286	324
31,148,163 – 31,148,318	D17S1833	154	154	154	154	154
33,160,167 – 33,160,320	D17S1788	156	160	160	160	156

Supplementary Figure S1-D: Analysis of microsatellite markers on chromosome 17 using DNA extracted from blood taken from patient 736 and hybrid cell lines #1 and #26 containing either the deletion-bearing or the normal chromosome 17 from the patient, respectively. Hybrid cell line #15 contains the wild-type chromosome 17 which was subject to the deletion in a number of cells. Patient 736 displays mosaicism for the type-2 *NF1* deletion. In peripheral blood, the deletion was detected in 94% of cells while 59% of her buccal smear cells had the deletion as determined by FISH [Kehrer-Sawatzki et al., 2004; Steinmann et al., 2007]. Marker alleles in parentheses displayed reduced signal intensity, indicative of somatic mosaicism involving both normal cells and cells bearing the deletion. The horizontal rectangular box includes those markers located within the deletion region. del: deletion of the allele. --: reduced signal intensity of markers which would have been indicative of somatic mosaicism but could not be formally assessed as a consequence of homozygosity. Nucleotide numbering is according to hg18, NCBI 36.

Position of marker on chromosome 17	Marker	Patient 1630 Blood		Hybrid #36	Father of patient 1630 Saliva		Mother of patient 1630 Saliva	
24,481,596 – 24,481,738	D17S1873	134	124	134	124	130	134	130
24,885,942 – 24,886,214	D17S1841	268	272	268	272	264	268	274
25,124,113 – 25,124,371	D17S975	258	254	258	254	262	258	254
26,497,479 – 26,497,687	D17S1307	210	--	210	210	200	210	210
26,594,230 – 26,594,438	D17S1849	207	--	207	207	207	207	207
26,641,851 – 26,642,254	D17S2237	404	(396)	404	396	400	404	400
26,664,798 – 26,665,027	IVs27TG24.8	272	--	272	272	280	272	272
26,668,420 – 26,668,626	IVs27AC28.4	207	--	207	207	207	207	213
26,673,142 – 26,673,342	D17S1166	194	--*	194	192	198	194	194
26,960,942 – 26,961,211	D17S1800	270	(278)	270	278	278	270	270
28,038,006 – 28,038,197	D17S1880	188	174	188	174	174	188	192
29,161,843 – 29,162,110	D17S1850	266	270	266	270	266	266	270
30,890,423 – 30,890,752	D17S907	336	304	336	304	286	336	304
31,148,163 – 31,148,318	D17S1833	154	154	154	154	156	154	154
33,160,167 – 33,160,320	D17S1788	156	156	156	156	156	156	156

Supplementary Figure S1-E: Analysis of microsatellite markers on chromosome 17 using DNA extracted from blood taken from patient 1630 and hybrid cell line #36 containing the wild-type chromosome 17 of the patient. Patient 1630 displays mosaicism for the type-2 *NF1* deletion. In peripheral blood, the deletion was detected in 92% of cells as determined by FISH [Steinmann et al., 2007]. The horizontal rectangular box includes those markers located within the deletion region. Marker alleles in parentheses displayed reduced signal intensity, indicative of somatic mosaicism involving normal cells and cells bearing the deletion.
--: reduced signal intensity of markers which would have been indicative of somatic mosaicism but could not be formally assessed as a consequence of homozygosity.
--*: a second allele was not visible, although heterozygosity was inferred form the paternal haplotype.
Nucleotide numbering is according to hg18, NCBI 36.

John Wiley & Sons, Inc.

Position of marker on chromosome 17	Marker	Patient 2358 Blood		Patient 2358 Buccal smear		Father of patient 2358 Buccal smear		Mother of patient 2358 Buccal smear		Brother of patient 2358 Buccal smear	
22,336,241 – 22,336,481	D17S783	247	241	n.d.	n.d.	247	241	241	251	247	251
24,481,596 – 24,481,738	D17S1873	140	142	n.d.	n.d.	140	120	142	126	140	126
24,885,942 – 24,886,214	D17S1841	272	272	n.d.	n.d.	272	264	272	272	272	272
25,124,113 – 25,124,371	D17S975	258	254	n.d.	n.d.	258	254	254	258	258	258
26,497,479 – 26,497,687	D17S1307	210	del	210	del	210	210	214	210	210	210
26,594,230 – 26,594,438	D17S1849	207	del	207	del	207	209	207	207	207	207
26,641,851 – 26,642,254	D17S2237	400	del	400	del	400	396	400	400	400	400
26,664,798 – 26,665,027	IVs27TG24.8	272	del	272	del	272	280	272	282	272	282
26,668,420 – 26,668,626	IVs27AC28.4	205	del	205	del	205	211	207	205	205	205
26,673,142 – 26,673,342	D17S1166	194	del	194	del	194	194	194	202	194	202
26,960,942 – 26,961,211	D17S1800	270	del	270	del	270	268	268	266	270	266
28,038,006 – 28,038,197	D17S1880	192	192	n.d.	n.d.	192	190	192	192	192	192
29,161,843 – 29,162,110	D17S1850	270	268	n.d.	n.d.	270	270	268	270	270	270
29,584,279 – 29,584,562	D17S1293	264	260	n.d.	n.d.	264	280	260	268	264	268
30,890,423 – 30,890,752	D17S907	340	286	n.d.	n.d.	340	286	286	286	340	286
31,148,163 – 31,148,318	D17S1833	154	156	n.d.	n.d.	154	156	156	156	154	156
33,160,167 – 33,160,320	D17S1788	156	156	n.d.	n.d.	156	166	156	166	156	166

Supplementary Figure S1-F: Analysis of microsatellite markers on chromosome 17 using DNA from blood samples and buccal mucosa taken from patient 2358 and family members. The horizontal rectangular box includes those markers located within the deletion region. del: deletion of the allele; n.d.: not determined.
Nucleotide numbering is according to hg18, NCBI 36.

Position of marker on chromosome 17	Marker	Patient 585 Blood,	Patient 585 Buccal smear	Father of 585 Blood		Mother of 585 Blood		Grandfather of 585 Blood		Grandmother of 585 Blood	
22,336,241 – 22,336,481	D17S783	246	246	246	240	246	246	246	272	246	246
24,481,596 – 24,481,738	D17S1873	140	140	140	130	140	124	124	136	140	142
24,885,942 – 24,886,214	D17S1841	268	272	268	270	272	272	n.d.	n.d.	272	272
25,124,113 – 25,124,371	D17S975	254	254	254	254	254	254	254	258	254	258
25,708,122 – 25,708,291	D17S1532	169	172	169	169	172	169	169	169	172	172
26,497,479 – 26,497,687	D17S1307	214	(206)	214	210	206	210	210	210	206	210
26,641,851 – 26,642,254	D17S2237	400	--	400	404	400	404	404	400	400	400
26,650,321 – 26,650,578	D17S2162	257	--	257	257	257	257	257	257	n.d.	n.d.
26,664,798 – 26,665,027	IVs27TG24.8	274	(272)	274	272	272	274	274	272	272	274
26,668,420 – 26,668,626	IVs27AC28.4	207	--	207	207	207	207	207	207	207	207
26,673,142 – 26,673,342	D17S1166	194	--	194	192	194	192	192	194	194	194
26,960,942 – 26,961,211	D17S1800	280	(276)	280	268	276	276	276	276	276	268
28,038,006 – 28,038,197	D17S1880	192	190	192	190	190	190	190	188	190	174
29,161,843 – 29,162,110	D17S1850	270	266	270	270	266	268	268	270	266	270
30,890,423 – 30,890,752	D17S907	320	286	320	300	286	286	286	300	286	300
31,148,163 – 31,148,318	D17S1833	164	156	164	158	156	154	154	154	156	154
33,160,167 – 33,160,320	D17S1788	156	162	156	156	162	156	156	166	162	156
40,162,539 – 40,162,644	D17S1861	96	104	96	90	104	102	102	104	104	104

Supplementary Figure S1-G: Analysis of microsatellite markers on chromosome 17 using DNA extracted from blood samples taken from patient 585 and her parents. Patient 585 has a mosaic type-2 *NF1* deletion. The horizontal rectangular box includes those markers located within the deletion region. n.d.: not determined. Marker alleles in parentheses displayed reduced signal intensity, indicative of somatic mosaicism involving both normal cells and cells bearing the deletion.
--: reduced signal intensity of markers which would have been indicative of somatic mosaicism but could not be formally assessed as a consequence of homozygosity.
Nucleotide numbering is according to hg18, NCBI 36.

Position of marker on chromosome 17	Marker	Patient 488 Blood		Hybrid #K1	Father of patient 488 Saliva		Mother of patient 488 Saliva	
22,336,241 – 22,336,481	D17S783	247	247	247	247	241	247	241
24,481,596 – 24,481,738	D17S1873	118	130	118	130	138	118	124
24,885,942 – 24,886,214	D17S1841	264	264	264	264	272	264	272
25,124,113 – 25,124,371	D17S975	254	254	254	254	254	254	258
25,708,122 – 25,708,291	D17S1532	172	169	172	169	169	172	169
26,497,479 – 26,497,687	D17S1307	210	del	210	210	210	210	206
26,594,230 – 26,594,438	D17S1849	207	del	207	207	207	207	207
26,641,851 – 26,642,254	D17S2237	400	del	400	400	400	400	400
26,652,321 – 26,650,578	D17S2162	258	del	258	258	258	258	258
26,664,798 – 26,665,027	IVs27TG24.8	272	del	272	272	272	272	272
26,668,420 – 26,668,626	IVs27AC28.4	207	del	207	207	207	207	213
26,673,142 – 26,673,342	D17S1166	194	del	194	192	194	194	194
26,960,942 – 26,961,211	D17S1800	282	del	282	266	276	282	270
28,038,006 – 28,038,197	D17S1880	174	190	174	190	192	174	192
29,161,843 – 29,162,110	D17S1850	266	268	266	268	270	266	270
29,584,279 – 29,584,562	D17S1293	264	272	264	272	288	264	264
30,890,423 – 30,890,752	D17S907	286	286	286	286	316	286	286
31,148,163 – 31,148,318	D17S1833	154	154	154	154	154	154	154
33,160,167 – 33,160,320	D17S1788	166	166	166	166	154	166	160
60,127,912 – 60,128,058	D17S1809	143	145	143	145	143	143	141

Supplementary Figure S1-H: Analysis of microsatellite markers on chromosome 17 using DNA from blood samples taken from patient 488. The proportion of cells harbouring the deletion was 98% in peripheral blood and 56% of buccal smear cells, as determined by FISH [Kehrer-Sawatzki et al., 2004; Steinmann et al., 2007]. The horizontal rectangular box includes those markers located within the deletion region. del: deletion of the allele.
Nucleotide numbering is according to hg18, NCBI 36.

Position of marker on chromosome 17	Marker	Patient 1502 Blood		Patient 1502 Buccal smear		Hybrid #KI.1-5	Father of patient 1502 Saliva		Mother of patient 1502 Saliva		Daughter of patient 1502 Blood	
24,481,596 – 24,481,738	**D17S1873**	130	124	n.d.	n.d.	124	130	136	124	134	130	136
24,885,942 – 24,886,214	**D17S1841**	274	272	n.d.	n.d.	272	274	264	272	272	274	270
25,124,113 – 25,124,371	**D17S975**	254	254	n.d.	n.d.	254	254	254	254	254	254	266
26,497,479 – 26,497,687	**D17S1307**	202	del	n.d.	n.d.	del	202	210	206	210	202	204
26,594,230 – 26,594,438	**D17S1849**	225	del	n.d.	n.d.	del	225	233	191	207	225	209
26,641,851 – 26,642,254	**D17S2237**	396	del	n.d.	n.d.	del	396	396	400	400	396	404
26,664,798 – 26,665,027	**IVs27TG24.8**	280	del	n.d.	n.d.	del	280	280	280	280	280	272
26,668,420 – 26,668,626	**IVs27AC28.4**	207	del	207	(205)	del	207	207	205	205	207	207
26,673,142 – 26,673,342	**D17S1166**	198	del	198	(202)	del	198	202	202	200	198	192
26,960,942 – 26,961,211	**D17S1800**	278	del	n.d.	n.d.	del	278	272	276	276	278	278
28,038,006 – 28,038,197	**D17S1880**	190	190	n.d.	n.d.	190	190	194	190	194	190	186
29,161,843 – 29,162,110	**D17S1850**	266	268	n.d.	n.d.	268	266	266	268	268	266	286
30,890,423 – 30,890,752	**D17S907**	286	324	n.d.	n.d.	324	286	316	324	316	286	316
31,148,163 – 31,148,318	**D17S1833**	154	164	n.d.	n.d.	164	154	154	164	154	154	154
33,160,167 – 33,160,320	**D17S1788**	156	156	n.d.	n.d.	156	156	159	156	159	156	160

Supplementary Figure S1-I: Analysis of microsatellite markers on chromosome 17 using DNA from patient 1502 and her family members as well as DNA extracted from somatic cell hybrid cells (hybrid #KI.1-5) containing only the deletion-bearing chromosome 17 from patient 1502. The proportion of cells harbouring the deletion was 97% in peripheral blood and 70% in buccal smear cells, as determined by FISH [Steinmann et al., 2007]. Marker alleles in parentheses displayed reduced signal intensity indicative of somatic mosaicism involving both normal cells and cells bearing the deletion. The horizontal rectangular box includes those markers located within the deletion region. del: deletion of the allele; n.d.: not determined.
Nucleotide numbering is according to hg18, NCBI 36.

Position of marker on chromosome 17	Marker	Patient 1956 Blood		Hybrid #FIII-1	Hybrid #FV-2-1	Hybrid #FV-4
24,481,596 – 24,481,738	D17S1873	138	124	124	124	138
24,885,942 – 24,886,214	D17S1841	264	272	272	272	264
25,124,113 – 25,124,371	D17S975	254	258	258	258	254
26,497,479 – 26,497,687	D17S1307	210	--	del	210	210
26,641,851 – 26,642,254	D17S2237	404	--	del	404	404
26,664,798 – 26,665,027	IVs27TG24.8	272	(280)	del	280	272
26,668,420 – 26,668,626	IVs27AC28.4	207	(209)	del	209	207
26,673,142 – 26,673,342	D17S1166	194	(202)	del	202	194
26,960,942 – 26,961,211	D17S1800	266	--	del	266	266
28,038,006 – 28,038,197	D17S1880	182	184	184	184	182
29,584,279 – 29,584,562	D17S1293	260	276	276	276	260
30,890,423 – 30,890,752	D17S907	286	316	316	316	286
31,148,163 – 31,148,318	D17S1833	154	154	154	154	154
33,160,167 – 33,160,320	D17S1788	156	156	156	156	156

Supplementary Figure S1-J: Analysis of microsatellite markers on chromosome 17 using DNA extracted from a blood sample from patient 1956 and hybrid cell lines containing only one chromosome 17 from the patient. Hybrid cell line #FIII-1 contains only the chromosome 17 harbouring the type-2 *NF1* deletion; hybrid cell line #FV-2-1 contains the wild-type chromosome 17 which was subject to the deletion in a number of cells. Hybrid cell line #FV-4 contains the wild-type chromosome 17 of the patient. In blood lymphocytes of patient 1956, 92% of the cells harboured the deletion as determined by FISH (in the present study). The horizontal rectangular box includes those markers located within the deletion region. Marker alleles in parentheses displayed reduced signal intensity, indicative of somatic mosaicism involving both normal cells and cells bearing the deletion.
--: reduced signal intensity of markers which would have been indicative of somatic mosaicism but could not be formally assessed as a consequence of homozygosity.
del: deletion of the allele.
Nucleotide numbering is according to hg18, NCBI 36.

Position of marker on chromosome 17	Marker	Patient IL39-III2 Blood		Hybrid #17 of IL39-III2	Hybrid #15 of IL39-III2	Patient IL39 (mother of IL39-III2) Blood		Father of patient IL39-III2 Blood		Grandmother of patient IL39-III2 Blood	
24,481,596 – 24,481,738	D17S1873	120	152	120	152	152	136	120	140	152	144
24,885,942 – 24,886,214	D17S1841	267	267	267	267	267	265	267	275	267	275
25,124,113 – 25,124,371	D17S975	255	263	255	263	263	259	255	255	263	259
26,594,230 – 26,594,438	D17S1849	235	del	235	del	--	211	235	211	211	237
26,673,142 – 26,673,342	D17S1166	195	del	195	del	--	195	195	203	195	303
26,960,942 – 26,961,211	D17S1800	276	del	276	del	--	276	276	268	276	268
28,038,006 – 28,038,197	D17S1880	178	196	178	196	196	186	178	194	196	196
30,890,423 – 30,890,752	D17S907	334	314	334	314	314	330	334	290	314	318
31,148,163 – 31,148,318	D17S1833	158	158	158	158	158	146	158	160	158	156
33,160,167 – 33,160,320	D17S1788	155	155	155	155	155	159	155	155	155	153
40,162,539 – 40,162,644	D17S1861	93	95	93	95	95	95	93	97	95	95

Supplementary Figure S1-K: Analysis of microsatellite markers on chromosome 17 using DNA extracted from blood from patient IL39-III2 and his family members. Patient IL39-III2 has a constitutional type-2 *NF1* deletion inherited from his mother (patient IL39) who is mosaic for a type-2 deletion as determined by FISH [Petek et al., 2003]. The deletion was observed in 70% of peripheral blood lymphocytes and 15% of fibroblasts from patient IL39. DNAs extracted from somatic cell hybrids containing only the chromosome 17 with the deletion of patient IL39-III2 (hybrid cell line #15) and from hybrids containing the wild-type chromosome from patient IL39-III2 (#17) were also analysed. The horizontal rectangular box includes those markers located within the deletion region. del: deletion of the allele. --: reduced signal intensity of markers which would have been indicative of somatic mosaicism but could not be formally assessed as a consequence of homozygosity.
Nucleotide numbering is according to hg18, NCBI 36.

Position of marker on chromosome 17	Marker	Patient 1104 Blood		Hybrid #KI.1	Hybrid #KI.2
22,336,241 – 22,336,481	D17S783	241	241	241	241
24,481,596 – 24,481,738	D17S1873	124	124	124	124
24,885,942 – 24,886,214	D17S1841	272	272	272	272
25,124,113 – 25,124,371	D17S975	258	254	258	254
25,708,122 – 25,708,291	D17S1532	169	169	169	169
26,497,479 – 26,497,687	D17S1307	210	(202)	210	202
26,594,230 – 26,594,438	D17S1849	207	(205)	207	205
26,664,798 – 26,665,027	IVs27TG24.8	274	(280)	274	280
26,673,142 – 26,673,342	D17S1166	194	(198)	194	198
26,960,942 – 26,961,211	D17S1800	276	(270)	276	270
28,038,006 – 28,038,197	D17S1880	190	174	190	174
30,890,423 – 30,890,752	D17S907	286	328	286	328
31,148,163 – 31,148,318	D17S1833	154	154	154	154
33,160,167 – 33,160,320	D17S1788	158	154	158	154

Supplementary Figure S1-L: Analysis of microsatellite markers on chromosome 17 using DNA from blood samples from patient 1104 as well as DNA extracted from somatic cell hybrids bearing the two wild-type chromosomes 17 of the patient. The deletion was observed in 84% of peripheral blood lymphocytes, 15% of urine cells and 8% of buccal smear cells from this patient [Steinmann et al., 2007]. Marker alleles in parentheses displayed reduced signal intensity, indicative of somatic mosaicism involving both normal cells and cells bearing the deletion. The horizontal rectangular box includes those markers located within the deletion region. Nucleotide numbering is according to hg18, NCBI 36.

Position of marker on chromosome 17	Marker	Patient 928 Blood		Hybrid #KI. 3	Hybrid #KI.1	Father of patient 928 Blood	
24,481,596 – 24,481,738	D17S1873	130	138	130	138	130	144
24,885,942 – 24,886,214	D17S1841	264	274	264	274	264	264
25,124,113 – 25,124,371	D17S975	254	258	254	258	254	254
26,497,479 – 26,497,687	D17S1307	210	del	210	del	210	210
26,614,084 – 26,614,348	NF1PCR3	266	del	n.d.	del	266	262
26,641,851 – 26,642,254	D17S2237	404	del	404	del	404	404
26,664,798 – 26,665,027	IVs27TG24.8	272	del	272	del	272	274
26,668,420 – 26,668,626	IVs27ac28.4	207	del	207	del	207	207
26,673,142 – 26,673,342	D17S1166	192	del	192	del	192	194
26,960,942 – 26,961,211	D17S1800	276	del	276	del	276	278
28,038,006 – 28,038,197	D17S1880	182	184	182	184	182	182
29,161,843 – 29,162,110	D17S1850	270	270	270	270	270	270
30,890,423 – 30,890,752	D17S907	323	286	323	286	323	286
31,148,163 – 31,148,318	D17S1833	154	154	154	154	154	156
33,160,167 – 33,160,320	D17S1788	166	166	166	166	166	154
40,162,539 – 40,162,644	D17S1861	102	102	102	102	102	102
60,127,912 – 60,128,058	D17S1809	145	141	145	141	145	145

Supplementary Figure S1-M: Analysis of microsatellite markers on chromosome 17 using DNA from blood samples from patient 928 and her father. DNA samples extracted from somatic cell hybrids carrying only the deletion-bearing chromosome 17 (hybrid #KI.1) or the wild-type chromosome (hybrid #KI.3) from patient 928 were also analysed. The deletion was observed in 80% of neurofibroma cells and 55% of buccal smear cells in patient 928 as determined by FISH [Kehrer-Sawatzki et al., 2004; Steinmann et al., 2007]. The horizontal rectangular box includes those markers located within the deletion region. del: deletion of the allele; n.d.: not determined. Nucleotide numbering is according to hg18, NCBI 36.

Position of marker on chromosome 17	Marker	Patient 2429 Blood		Patient 2429 Buccal smear		Hybrid #KI.1-5	Father of patient 2429 Blood		Mother of patient 2429 Blood		Brother of patient 2429 Blood	
24,481,596 – 24,481,738	D17S1873	134	130	n.d.	n.d.	134	134	140	130	126	140	126
24,885,942 – 24,886,214	D17S1841	278	272	n.d.	n.d.	278	278	272	272	272	n.d.	n.d.
25,124,113 – 25,124,371	D17S975	258	254	n.d.	n.d.	258	258	258	254	258	258	258
26,497,479 – 26,497,687	D17S1307	del	206	n.d.	n.d.	del	210	210	206	210	210	210
26,641,851 – 26,642,254	D17S2237	del	400	n.d.	n.d.	del	400	404	400	396	404	396
26,664,798 – 26,665,027	IVs27TG24.8	del	274	del	274	del	272	280	274	280	280	280
26,668,420 – 26,668,626	IVs27AC28.4	del	207	del	207	del	203	205	207	209	205	209
26,673,142 – 26,673,342	D17S1166	del	194	del	194	del	192	202	194	202	202	202
26,960,942 – 26,961,211	D17S1800	del	276	n.d.	n.d.	del	278	276	276	272	276	272
28,038,006 – 28,038,197	D17S1880	192	174	n.d.	n.d.	192	174	192	174	192	192	192
30,890,423 – 30,890,752	D17S907	328	316	n.d.	n.d.	328	300	328	316	312	328	312
31,148,163 – 31,148,318	D17S1833	154	156	n.d.	n.d.	154	156	154	156	154	154	154
33,160,167 – 33,160,320	D17S1788	166	160	n.d.	n.d.	166	160	166	160	156	160	156
40,612,539 – 40,162,644	D17S1861	108	96	n.d.	n.d.	108	106	108	96	104	106	104
60,127,912 – 60,128,058	D17S1809	142	138	n.d.	n.d.	142	140	142	138	144	140	138

Supplementary Figure S1-N: Analysis of microsatellite markers on chromosome 17 using DNA from blood samples from patient 2429 and his family members as well as DNA extracted from hybrid cell line #KI.1-5 containing only the chromosome 17 with the deletion from patient 2429. In the brother of patient 2429, a crossover between markers D17S1833 and D17S1788 has to be assumed on the paternal chromosome whilst a crossover between markers D17S1861 and D17S1809 on the maternal chromosome has to be assumed to explain the observed haplotypes. The horizontal rectangular box includes those markers located within the deletion region. del: deletion of the allele; n.d.: not determined.
Nucleotide numbering is according to hg18, NCBI 36.

Position of marker on chromosome 17	Marker	Patient SB Blood		Hybrid #S10	Hybrid #B9	Patient WB (Mother of patient SB) Blood		Sister of patient SB Blood	
24,481,596 – 24,481,738	D17S1873	130	134	130	134	134	126	126	130
24,885,942 – 24,886,214	D17S1841	266	278	266	278	278	272	272	266
25,124,113 – 25,124,371	D17S975	264	260	264	260	260	260	260	264
26,497,479 – 26,497,687	D17S1307	214	del	214	del	del	206	206	214
26,594,230 – 26,594,438	D17S1849	209	del	209	del	del	207	207	209
26,641,851 – 26,642,254	D17S2237	400	del	400	del	del	400	400	400
26,664,798 – 26,665,027	IVs27TG24.8	272	del	272	del	del	272	272	272
26,668,420 – 26,668,626	IVs27AC28.4	209	del	209	del	del	213	213	209
26,673,142 – 26,673,342	D17S1166	194	del	194	del	del	194	194	194
28,038,006 – 28,038,197	D17S1880	174	182	174	182	182	182	182	174
29,584,279 – 29,584,562	D17S1293	284	276	284	276	276	284	284	284
30,890,423 – 30,890,752	D17S907	324	324	324	324	324	320	320	324
31,148,163 – 31,148,318	D17S1833	154	154	154	154	154	154	154	154
33,160,167 – 33,160,320	D17S1788	160	156	160	156	156	156	156	160
40,162,539 – 40,162,644	D17S1861	102	102	102	102	102	92	92	102

Supplementary Figure S1-O: Analysis of microsatellite markers on chromosome 17 using DNA from blood samples from patient SB and her family members as well as DNA extracted from somatic cell hybrids #S10 and hybrid #B9 containing respectively only the wild-type chromosome 17 and only the deletion-bearing chromosome 17 from patient SB. The horizontal rectangular box includes those markers located within the deletion region. Patient SB has a germline type-2 *NF1* deletion inherited from her mother (patient WB) who exhibited somatic mosaicism for the deletion. The deletion was observed in 94% of blood cells from patient WB, as determined by FISH [Kehrer-Sawatzki et al., 2004; Steinmann et al., 2007]; del: deletion of the allele.
Nucleotide numbering is according to hg18, NCBI 36.

Position of marker on chromosome 17	Marker	Patient UC172 Blood		Hybrid #1	Hybrid #2	Father of patient UC172 Blood		Mother of patient UC172 Blood	
22,336,241 – 22,336,481	D17S783	243	241	243	241	243	251	241	241
24,481,596 – 24,481,738	D17S1873	138	124	138	124	138	124	124	130
24,885,942 – 24,886,214	D17S1841	270	266	270	266	270	276	266	270
25,124,113 – 25,124,371	D17S975	252	256	252	256	252	252	256	252
25,708,122 – 25,708,291	D17S1532	175	173	175	173	175	175	173	173
26,497,479 – 26,497,687	D17S1307	208	--	208	del	208	208	208	208
26,594,230 – 26,594,438	D17S1849	207	--	207	del	207	207	207	209
26,641,851 – 26,642,254	D17S2237	404	--	404	del	404	408	404	404
26,664,798 – 26,665,027	IVs27TG24.8	272	--	272	del	272	280	272	272
26,668,420 – 26,668,626	IVs27AC28.4	203	(205)	203	del	203	205	205	205
26,673,142 – 26,673,342	D17S1166	192	--	192	del	192	202	192	192
26,960,942 – 26,961,211	D17S1800	270	(268)	270	del	270	268	268	276
28,038,006 – 28,038,197	D17S1880	190	192	190	192	190	198	192	188
29,161,843 – 29,162,110	D17S1850	266	270	266	270	266	270	270	270
29,584,279 – 29,584,562	D17S1293	278	276	278	276	278	280	276	276
30,890,423 – 30,890,752	D17S907	328	320	328	320	328	286	320	286
33,160,167 – 33,160,320	D17S1788	156	160	156	160	156	160	160	160
60,127,912 – 60,128,058	D17S1809	145	143	145	143	145	143	143	141

Supplementary Figure S1-P: Analysis of microsatellite markers on chromosome 17 using DNA from blood samples from patient UC172 and her family members as well as DNA extracted from somatic cell hybrids #1 and #2 containing only the wild-type chromosome 17 and only the deletion-bearing chromosome 17 from patient UC172, respectively. The deletion was observed in 86% of blood cells from this patient as determined by FISH (this study). The horizontal rectangular box includes those markers located within the deletion region. Marker alleles in parentheses displayed reduced signal intensity, indicative of somatic mosaicism involving normal cells and cells bearing the deletion.

--: reduced signal intensity of markers which would have been indicative of somatic mosaicism but could not be formally assessed as a consequence of homozygosity. del: deletion of the allele.

Nucleotide numbering is according to hg18, NCBI 36.

Position of marker on chromosome 17	Marker	Patient 938 Blood		Hybrid del	Mother of patient 938 Blood		Father of patient 938 Blood	
24,481,596 – 24,481,738	D17S1873	118	140	140	140	144	118	130
24,693,853 – 24,694,013	D17S2093	160	160	160	160	160	160	160
24,885,942 – 24,886,214	D17S1841	264	272	272	272	272	264	272
25,124,113 – 25,124,371	D17S975	258	254	254	254	272	258	258
25,708,122 – 25,708,291	D17S1532	169	169	169	169	169	169	169
26,594,230 – 26,594,438	D17S1849	207	(229)	del	229	207	207	233
26,641,851 – 26,642,254	D17S2237	400	--	del	400	404	400	404
26,664,798 – 26,665,027	IVs27TG24.8	272	--*	del	274	280	272	280
26,668,420 – 26,668,626	IVs27AC28.4	213	(207)	del	207	207	213	213
26,673,142 – 26,673,342	D17S1166	194	(202)	del	202	194	194	202
26,960,942 – 26,961,211	D17S1800	276	--*	del	268	270	276	280
28,038,006 – 28,038,197	D17S1880	196	190	190	190	190	196	192
30,890,423 – 30,890,752	D17S907	286	286	286	286	312	286	316
31,148,163 – 31,148,318	D17S1833	154	156	156	156	154	154	154
33,160,167 – 33,160,320	D17S1788	166	166	166	166	156	166	166
60,127,912 – 60,128,058	D17S1809	145	149	149	149	145	145	147

Supplementary Figure S1-Q: Analysis of microsatellite markers on chromosome 17 using DNA from blood samples from patient 938 and her family members as well as DNA extracted from a somatic cell hybrid containing only the chromosome 17 bearing the deletion of patient 938. The deletion was observed in 91% of peripheral blood lymphocytes and 80% of buccal smear cells in patient 938 as determined by FISH [Kehrer-Sawatzki et al., 2004; Steinmann et al., 2007]. Marker alleles in parentheses were visible as peaks with strongly reduced signal intensity, indicative of somatic mosaicism involving normal cells and cells bearing the deletion. The horizontal rectangular box includes those markers located within the deletion region.
--: reduced signal intensity of markers which would have been indicative of somatic mosaicism but could not be formally assessed as a consequence of homozygosity. --*: a second allele was not visible, although heterozygosity was inferred form the maternal haplotype.
del: deletion of the allele.
Nucleotide numbering is according to hg18, NCBI 36.

John Wiley & Sons, Inc.

Position of marker on chromosome 17	Marker	Patient HC Blood		Patient HC Buccal smear		Hybrid #KI.1	Hybrid #KI.6	Father of patient HC Blood		Mother of patient HC Blood	
22,336,241 – 22,336,481	**D17S783**	241	239	n.d.	n.d.	239	241	241	241	239	239
24,481,596 – 24,481,738	**D17S1873**	136	144	n.d.	n.d.	144	136	136	130	144	130
24,885,942 – 24,886,214	**D17S1841**	270	272	n.d.	n.d.	272	270	270	272	272	264
25,124,113 – 25,124,371	**D17S975**	254	258	n.d.	n.d.	258	254	254	258	258	262
25,708,122 – 25,708,291	**D17S1532**	163	163	n.d.	n.d.	163	163	163	169	163	173
26,594,230 – 26,594,438	**D17S1849**	207	--	n.d.	n.d.	del	207	207	233	207	207
26,614,048 – 26,614,348	**NF1PCR3**	266	--*	n.d.	n.d.	del	266	266	262	262	274
26,641,851 – 26,642,254	**D17S2237**	404	--	n.d.	n.d.	del	404	404	400	404	404
26,668,420 – 26,668,626	**IVs27AC28.4**	213	--*	213	(207)	del	213	213	209	207	207
26,960,942 – 26,961,211	**D17S1800**	268	--*	268	(276)	del	268	268	280	276	280
28,038,006 – 28,038,197	**D17S1880**	188	174	n.d.	n.d.	174	188	188	188	174	174
30,890,423 – 30,890,752	**D17S907**	314	286	314	286	286	314	314	324	286	324
31,148,163 – 31,148,318	**D17S1833**	162	156	n.d.	n.d.	156	162	162	154	156	154
33,160,167 – 33,160,320	**D17S1788**	154	164	n.d.	n.d.	164	154	154	154	164	154

Supplementary Figure S1-R: Analysis of microsatellite markers on chromosome 17 using DNA from blood samples from patient HC and his parents. DNAs derived from somatic cell hybrids either carrying the chromosome 17 with the deletion (hybrid #KI.1) or bearing the wild-type chromosome 17 of patient HC (hybrid # KI.6), were also analysed. The horizontal rectangular box includes those markers located within the deletion region. Marker alleles in parentheses displayed reduced signal intensity indicative of somatic mosaicism involving both normal cells and cells bearing the deletion.
--: reduced signal intensity of markers which would have been indicative of somatic mosaicism but could not be formally assessed as a consequence of homozygosity.
--*: a second allele was not visible, although heterozygosity was inferred form the maternal haplotype.
del: deletion of the allele. n.d.: not determined.
Nucleotide numbering is according to hg18, NCBI 36.

For Peer Review

Supplementary Figure S2: Non-B DNA-forming repeats in the breakpoint-spanning regions, also termed recombination regions (RRs; grey), of the 16 type-2 *NF1* deletions mediated by NAHR. Sequences flanking the RRs in a proximal direction are marked in yellow. Sequences flanking the RRs in a telomeric direction are marked in blue. Paralogous sequence variants are highlighted in bold. Direct repeats are shown in pink or red letters. Inverted repeats are highlighted in green. Symmetric repeats are underlined. Inverted repeats capable of non-B DNA structure formation were found to be overrepresented within the RRs (p<0.001) whereas both direct and inverted repeats were overrepresented within the extended RRs (p<0.001). Extended RRs also encompass 100 bp in centromeric and telomeric directions, marked in yellow and blue, respectively.
Nucleotide numbering is according to hg18, NCBI 36.

Patient 811-M

```
AGTTGAATACAATAAATAGCTCTTTTTTGGCCAGGCATGGTGGCTCACAC   26,093,051-26,093,100
CTTTAATCCTAGCACTTTGGGAGACAGGGGTGGATAGATCACCTGAGGTC   26,093,101-26,093,150
AGGAGTTCAAGACCAGCCTGACCAACATGGTGAAACCCTGTCTCTA.      26,093,151-26,093,196
                                                    (27,297,456-27,297,501)
CAAAATGCAAAAATTAGCCAGGCGTGGTGGTGCACACCTGTAGTCCCAGC   27,297,502-27,297,551
TACTCGGGAGGCTGAGGCAGGAGAATTGCCTGAACCCGGGAGGTGGAGGT   27,297,552-27,297,601
```

Patient KCD

```
GCTTGGGTGGTGTTTGTTCATTCATTAACTACCTTTAGAGAGAATGCAGA   26,095,211-26,095,260
ACTAAAAATATTAGATTCTTAAAAAAATAGAGTTGGAAAATTTGTCACAG   26,095,261-26,095,310
TGCATTTTTCTTTTCCTTCTAGTTTTAAATCACAGCTTACGAATTTAGAT   26,095,311-26,095,419
AGGATACACACTTAATGATGCATCATTTATGCATCTCATTGTTTTCCCAT  (27,299,613-27,299,721)
TGTTCTGTT
GACTGGTAAAAGACTTCCTTTTTTCAGTTTGGCTTCCTTCTATTTTAAG   27,299,722-27,299,771
TTTGGCTTTGGAATTAAGTGATTTTTTTACTTGGATTATAAAATGATATT   27,299,772-27,299,821
```

Patient 697

```
CCATGCCTGGCCTTATTTTTATTTTTTGAGACAAGGTCTCGCTTTGTCAC   26,100,213-26,100,262
CGAGGCTGGAGTGTAGTGGCATAATGATAGGTCACTGATGGATTGAACTC   26,100,263-26,100,312
GTGGACTAAAGGGATCCTCCTGCCTCAGCCTCCTGAGTAGCTGGGACTAC   26,100,313-26,100,381
AGGCATGTACTGTCACACC                                 (27,304,631-27,304,699)
TCACTAATTTTTTGAATTTTTGTAGAGTCAGGGTCTCATCATCTTGCCCA   27,304,700-27,304,749
GGCCAGTTTTGAACTCCTATCCTCAAGTGATCCTCCCACCTCGACATCCT   27,304,750-27,304,799
```

Patient 736

```
AGCCTCCCAAAGCGCTGGGATTATAGCCGTGAGCCACTGCCCCCAGCCGG   26,104,491-26,104,540
TTTTTGTATTTTTAGCAGAGACGGAGTTTCACCATGTTGGCCAGGCTGGT   26,104,541-26,104,590
CTCGAATTCTTGACCTCAAGTTATCCACCAGCCTCAGCCTCCCAAAGTGC   26,104,591-26,104,678
TGGATTACAGGTGTGAGCCACTGCACCTGGCCCTGGAT             (27,308,895-27,308,982)
TACAGGTGTGAGCCACTGCACCTGGCCCTGGCTCACCTTTTGTCCTTTTT   27,308,983-27,308,982
TTTTTTTTTTTTTTTTTTTTGAGACAGAGTCTTGCTCTGTCGCCCAGGCT   27,309,033-27,309,082
```

Patient 1630

```
TTATCTTATGAAAAAAATTTGTTGGGTCATTTTCTGTAAGACACTGCTAG   26,108,723-26,108,772
GTGCTAGGGACACTAATAAAAAGATGTATATGGAAAAATAGTGACTAAAC   26,108,773-26,108,822
AGTGGTAAATAAGAGTGCTTGTAAAGGGATAAAGTGGTCATTTAGCTCTT   26,108,823-26,108,934
GATTGATTGGGTTTAGGGTCTTTGTAGAAGAGGGAGAGAGTATTTTGCTG  (27,313,160-27,313,271)
GATACTTTATTA
TTTTCTGCAAGCCTGACCAGGCACAGTGGCTCATGCCTATAATCGCAGCA   27,313,272-27,313,321
CTTGGGGAGGCTGAGGTGGGATGATCACTTGCACCCAGGAGTTCATTACC   27,313,322-27,313,371
```

Patient 2358

```
GTTATGAATGTCTCCTGATCAACAGCTGTATTCTGTTTTGCAGTTTAAAG  26,109,815-26,109,864
GTACTTCAAAAGCTTATTGGTGCTTCTGTTTGTTTTATCCCATCCTTATA  26,109,865-26,109,914
GTTTTTTTCTATTGTTAATAGATGTTTGTGAAAATAGAAGGAGCACTAGT  26,109,915-26,109,978
TCTAGTTCATGCTT                                     (27,316,556-27,316,619)
GCTTTTGCTTTTCCATAGCTTCTAAAACTAACAGTGAAAATGATATATTG  27,316,620-27,316,669
AAACAGTAAATTATAGATCTATACCAGATTTGTAATTGTGTATTTCATTG  27,316,670-27,316,719
```

Patient 585

```
ATTGGTGCTTCTGTTTGTTTTATCCCATCCTTATAGTTTTTTTCTATTGT  26,109,880-26,109,929
TAATAGATGTTTGTGAAAATAGAAGGAGCACTAGTTCTAGTTCATGCTTT  26,109,930-26,109,979
CTTTTGCTTTTCCATAGCTTCTAAAACTAACAGTGAAAATGATATATTGA  26,109,980-26,110,109
AACAGTAAATTATAGATCTATACCAGATTTGTAATTGTGTATTTCATTGC (27,316,621-27,316,750)
TATTTGAAGTATAAAGTAATGGTTCTGTAT
CATTTATTGGGAAGGTTGAATTTCCATAGCTTCAAAATATTCAAATTTTT  27,316,751-27,316,800
TTGCATGGATTTAGCTACGCTTTTCAAAATTTCCTTTTGATGAAGTCATT  27,316,801-27,316,850
```

Patient 488

```
TTGGAAGGCTGAGGCGGGTGTATCATGACCCCAGGAGTTCAGGACCAGCC  26,111,449-26,111,498
TGGCCAATATGGTGAAACCCCATCTCTACTAAAAATATAAACATTAGCCG  26,111,499-26,111,548
GGCGTGGTGGTGGGTGCCTGTAGTCCCAGTTACTTGGGAGACTTAGGCAG  26,111,549-26,111,605
AAGAATC                                            (27,318,189-27,318,245)
ACTTGAACCTGAGAGTCGGAGGTTGCAATGAGCTGAGATTGCGTTACTGC  27,318,246-27,318,295
ACTCCAGCCTGGGCGACAGAGCGAGACTCCATCTCAAAAAAAAAAAAAAA  27,318,296-27,318,345
```

Patient 1502

```
TGAGAGTCAGAGGTTGCAGTGAGCTGAGATTGTGTTACTGCACTGCAGCC  26,111,615-26,111,664
TGGGCGACAGAGCGAGACTCCATCTCAGAAAAAAAAGGGGGGGGAAAATT  26,111,665-26,111,714
ACTTATCAGCTTATCCATCATAAGTCTGTGTATATGGCATATATTTTTAT  26,111,715-26,111,905
TATGCAATGGAATAAAACCATTATTAGAAACATGCCAGGTTGGTTGTCTT (27,318,355-27,318,545)
GGTATCGTTTAGTAAGAAACAAAGATTGAAAATGAGTCCTGGTGGGCCGG
GCACGGTGGCTCACGCCTGTAATCCCAGCACTTTGGGAGGC
TGAGGCGGGTGGATCACAAGGTCAGGAGATCGAGACTATCCTGGCTAACA  27,318,546-27,318,595
TGGTGAAACCCCGTCTCTACTAAAATACAAAAAAACTAGCTGGGTGTCGT  27,318,596-27,318,645
```

Patient 1956

```
GCTTGGGCAACACAGACCCCATCTCTACAAAAATTAGCCAGGTATGGTGG  26,112,265-26,112,314
GTATGTCCTGTAGTTCTAGGTACTTGGAAGTCCAAGATGGCAGGATGGCA  26,112,315-26,112,364
TAAGCTCAGGAATTCAAGGTTACAGTTACCTATGATTGCACAACTCTACT  26,112,365-26,112,510
CCAGGCTGGGCAACAGAGTGAGACTCTGTCTCCAAAAAATCCCAAATATT (27,318,916-27,319,061)
AGACTGGGCATGGTGGCTCACAGCTATAATGTCAACACCTTGGGAG
GCTGAGATGGAAGAATAGCTTGAGGCTTGCCTGGGCAACATAGGGAGAAC  27,319,062-27,319,111
CTGTCTGTAAGAAGTAAAAAAAGATTAACTGGGCACAGTGGCACATGCCT  27,319,112-27,319,161
```

Patient IL39

```
GTTGCCCAATGCCTTAGAACAAAAATTTTTTTTTGTATGTTCATGGATTC  26,115,406-26,115,455
ATCTATTATAATAGTTCTGGATGTTATTGAAGCTATTTGATGAATTATTT  26,115,456-26,115,505
ATTAAATATTCAGTTATGAACTGTTAATACCTTTGGGACTTTAAAAA     26,115,506-26,115,552
                                                   (27,322,062-27,322,108)
CAAGTTATGGAGGACTACTCTAGAACCTTAATTTGTAAAGCCTGTGTTAA  27,322,109-27,322,158
TTTACATAGAGAATATAGACTATGGTATTCAAAATTAACACCCCTAAATT  27,322,159-27,322,208
```

Patient 1104

```
ATTTATTAAATATTCAGTTATGAACTGTTAATACCTTTGGGACTTTAAAA  26,115,502-26,115,551
AAAAGTTATGGAGGACTACTCTAGAACCTTAATTTGTAAAGCCTTTGTTA  26,115,552-26,115,601
GTTAATTTACATAGAGAATATAGACTATGGTATTCAAAATTAACACCCCT  26,115,602-26,115,677
AAATTTTTTGTAAGCCAAGATATTCT                         (27,322,154-27,322,229)
AGATAGTAAATAATATCTTGATTTTTGTTATCCCATTTAAACTGTAGAGA  27,322,230-27,322,279
AATTCTGGGGAAAGCATCTAAAAATAGCTCTGATAGCTCTGTCTCTACGT  27,322,280-27,322,329
```

Patient 2429

```
TACCATGCCCAGCTAATTTTTGTGTTTTTAGAGAGATGAGGTTTCACCAT  26,122,847-26,122,896
GTTGGCCAGGCTGGTCTGGAGCTCCTGACCTCACATCATCCACCTGCCTA  26,122,897-26,122,946
AGCCTCCCAAAGTGCTGGGATTACAGGTGAGCCACCGTGCCCGGCCAGTG  26,122,947-26,123,171
TCTTTTTAAAGTCAGAAATTTTATTGTGGATCGAAGATTTAAATGGAAAA (27,329,593-27,329,817)
CAATAGAACCATAAATGTACTAGAAAATAGTGGTCATGTCTGTGGGGGAA
ACAATTAGAATGAGGCGCATTGGACTTCATCGATGCTGTTAATTGTTCTA
TTTTAGGCAGCATGGGGTATGTTCT
ATTTTCTTTTTAATCACTGTACCTGACACATATGTTTACACATTTCTTG  27,329,818-27,329,867
TAAGAAAAAGATAATGCTTTTATTTTAAAGAAAAAGTGCCAAGAAGAAAC  27,329,868-27,329,917
```

Patients WB and UC172

```
TCAGGCTGGTCTTGAACTCCCGACCTCAGGTGATCCTCCCACCTCAGCCT  26,125,130-26,125,179
CCCGAAGTGTGGGGATTACGGGCATGAGCCACTGCGTCGGGCCAACCTTC  26,125,180-26,125,229
TCTTACCTCTGCTCTGAAGTTGTGATTTCTTCAAGGAGTCCTGATTCCTT  26,125,230-26,125,406
ATAGAAGAATAGTATTTTTAAGCCAAAATCTGCATGTTAGATGTGTAAAA (27,331,894-27,332,070)
ATTGTTTTTAAAATCTCACAGAGGGCTGAGTGCAGTGGCTCACACTTGTA
ATCTTAGTACTTTGGAAGACCAAGGTG
AGAGGATCTCTTGAGCCCAGGAGTCTGAGGCTGTAGTGAGCTATGATTGT  27,332,071-27,332,120
GTCACTGCACTCTAGCCTGGGTGACACAGCGACTGTCAAAAAAAAAAACC  27,332,121-27,332,170
```

Patient 938

```
GCTATGGACTACTTAGAAGGTTGAGCACATTATAGTTATGAACTCCCATT  26,127,546-26,127,595
TTTGATTGATGTTTTCTTCCCCAAATGCTAATTCATGTTGGAAGTAGAGG  26,127,596-26,127,645
CCTTTGTTTTTTATACTTTAAAAAACACAAGTAAATGATCTAGTCAGAGC  26,127,646-26,127,756
ATTTAACGGAAGGTATCATTCCTTTTTTTTTTTTTTTTTGAGGGGGAGT (27,334,336-27,334,446)
CTTGCTCTGT T
GCCCAGGCTGGAGTGCAGTGGCATGGTCTCGGCTCACTGCAACCTCCACC  27,334,447-27,334,496
TCCCGGGTTCAAGCGATTCTCCTGTCTCAGCCTCCCAAGTAGCTGTGATT  27,334,497-27,334,546
```

For Peer Review

Supplementary Table S1: Methods used to identify the type-2 deletion breakpoints in 18 NF1 patients

Patient	Methods used to identify the deletion breakpoints
811-M[a]	Breakpoint-spanning PCR on genomic DNA based on SNP array results
KCD[b]	Sequence analysis of PCR products amplified from somatic cell hybrids containing only the chromosome 17 with the deletion
697[a]	Sequence analysis of PCR products amplified from somatic cell hybrids containing only the chromosome 17 with the deletion
736[a]	Breakpoint-spanning PCR on genomic DNA based on SNP array results
1630[a]	Breakpoint-spanning PCR on genomic DNA based on SNP array results
2358[c]	Breakpoint-spanning PCR on genomic DNA based on SNP array results
585[c]	Breakpoint-spanning PCR on genomic DNA based on SNP array results
488[a]	Breakpoint-spanning PCR on genomic DNA based on SNP array results
1502[a]	Sequence analysis of PCR products amplified from somatic cell hybrids containing only the chromosome 17 with the deletion
1956[c]	Sequence analysis of PCR products amplified from somatic cell hybrids containing only the chromosome 17 with the deletion
IL39[b]	Sequence analysis of PCR products amplified from somatic cell hybrids containing only the chromosome 17 with the deletion
1104[a]	Breakpoint-spanning PCR on genomic DNA based on SNP array results
928[a]	Sequence analysis of PCR products amplified from somatic cell hybrids containing only the chromosome 17 with the deletion
2429[c]	Sequence analysis of PCR products amplified from somatic cell hybrids containing only the chromosome 17 with the deletion
WB[b]	Sequence analysis of PCR products amplified from somatic cell hybrids containing only the chromosome 17 with the deletion
938[a]	Sequence analysis of PCR products amplified from somatic cell hybrids containing only the chromosome 17 with the deletion
HC[a]	Sequence analysis of PCR products amplified from somatic cell hybrids containing only the chromosome 17 with the deletion
UC172[c]	Sequence analysis of PCR products amplified from somatic cell hybrids containing only the chromosome 17 with the deletion

[a] breakpoints were identified as previously described [Steinmann et al. 2007]
[b] breakpoints as determined in Kehrer-Sawatzki et al. [2004].
[c] breakpoints were identified in the present study.

John Wiley & Sons, Inc.

Supplementary Table S2: Clinical features of the five newly identified type-2 *NF1* deletion patients

Patient	Sex (age in years)	Clinical features
2358	f (10)	Multiple CALM, axillary and inguinal freckling, hypotony, hypertelorism, plexiform neurofibroma on the right calf, no dermal neurofibromas, no spinal or intra-abdominal tumours as determined by MRI, T2 hyperintensities in the cerebellum, mild developmental delay, attends primary school.
585	f (7)	Multiple CALM, axillary and inguinal freckling, plexiform neurofibroma on the neck, no intellectual disabilities or psychomotor developmental delay.
1956	m (9)	More than 6 CALM, axillary freckling, Lisch nodules, scoliosis, no neurofibromas, attends primary school but is behind normal educational level for age, no significant developmental delay or dysmorphic facial features.
2429	m (16)	Multiple CALM, axillary and inguinal freckling, Lisch nodules, height 182cm; head circumference 60cm, one MPNST, congenital heart disease, >1000 subcutaneous neurofibromas, ~ 500 cutaneous neurofibromas, plexiform neurofibromas on face and neck, corpus callosum aplasia, IQ 84, learning problems, hypertelorism, saddle nose, dysmorphic facial features, large hands and feet, hyperflexibility of joints, funnel chest, broad neck.
UC172	f (6)	Multiple CALM, axillary and inguinal freckling, no dermal or subcutaneous neurofibromas, no intellectual disabilities or psychomotor developmental delay.

CALM: Cafe-au-lait macules
MPNST: malignant peripheral nerve sheath tumour

For Peer Review

Supplementary Table S3: Primers used to investigate the presence of a duplication reciprocal to the respective type-2 *NF1* deletion

Patient	PCR-product (bp)	Primer	Position [a]	Primer 5' → 3' [b]
811	914	D-F1	27,297,148-27,297,172	GCgCTTCTTACTATACTCTATTGGA
		D-R2	26,093,737-26,093,756	TGATCCATCAAATCG---cAAAA
	873	D-F1/2	27,297,189-27,297,220	AAGTTTTCAGTAACTCTAAAGGTAAAGAGAGA
		D-R2/2	26,093,736-26,093,756	TGATCCATCAAATCG---cAAAAC
KCD	438	D-F3	27,299,533-27,299,559	TCATTCATTAACT-CCTTTAGAGAG--TGC
		D-R4	26,095,648-26,095,668	CCCTGGGCATTAACAGATgTA
	904	D-F3/2	27,299,532-27,299,558	CATTCATTCATTAACT-CCTTTAGAGAG--TG
		D-R4/2	26,096,112-26,096,135	cTTTGAGTTGCTATTGAACCACTG
697	2,024	D-F5	27,303,631-27,303,655	TgGTATATGCTAGCAGGATTCTAGG
		D-R6	26,101,315-26,101,334	TACGGAAATGAAACGTGCAA
736	4,673	D-F7	27,306,085-27,306,107	TTGGTCTTAAGAAAGTCGTTTGT
		D-R8	26,106,439-26,106,456	CTGCTAGCgGCAGGcATA
1630	1,398	D-F9	27,312,802-27,312,830	GTTGTTAGTAGTAgTCTCAAtTTCTTGAG
		D-R10	26,109,839-26,109,862	TTAAACTGCAAAACAgAATACAGc
	909	D-F9/2	27,312,386-27,312,411	gATAATGGCTGGTTGGCTGGGCatAg
		D-R10/2	26,108,935-26,108,957	TGCGCAGTCAGGCTTGCAGAAAG
585	668	NJ7f	27,316,459-27,316,480	ATGAATGTCTCCTGATCAACAa
		NJ8r	26,110,458-26,110,483	CCTGTTAAATATGACATCCAAAAGTt
488/ 1502	2,608	D-F11/2	27,317,289-27,317,308	CATTTGCAGCTTACGTTTAC
		D-R12	26,113,233-26,113,256	ATAATTTAAGGAAAACAAAAAtCa
1956	1,436	D-F13	27,318,373-27,318,397	CATAAGTCTGTGTATATGGCATATc
		D-R14	26,113,233-26,113,257	AATAATTTAAGGAAAACAAAAAtCa
IL39/ 1104	1,610	D-F15	27,320,718-27,320,739	CGCCTATGTTGAAAATAACTat
		D-R16	26,115,749-26,115,770	CGTAGAGA--------CAGAGCTATTTTTA
	427	D-F15/2	27,322,040-27,322,061	GAAGCTATTTGATGAATTAgTg
		D-R16/2	26,115,891-26,115,914	AACATTTGAATTAAATCAGTTACt
WB/ UC172	3,320	D-F19	27,329,085-27,329,109	GGCAAGAAACACAGACtTATtAAat
		D-R20	26,125,718-26,125,740	CATTCTTCTATTGGGCA----aC-TTTA
	531	D-F19/2	27,331,874-27,331,893	cCcGGCCtACCTTCTTCTTt
		D-R20	26,125,718-26,125,740	CATTCTTCTATTGGGCA----aC-TTTA
938	2,257	D-F21	27,333,149-27,333,171	TGGTTGAAGAATGGTGTTTAGAG
		D-R22	26,128,656-26,128,679	ACACCTTTATCAT-AAACTATTTCA

a: according to the human genome assembly hg18, NCBI 36

b: Primers bind to regions of sequence divergence between the *SUZ12* gene and its pseudogene *SUZ12P*. The forward primer has been designed according to the sequence of the *SUZ12* gene, whereas the reverse primer has been designed according to the sequence of *SUZ12P*. Nucleotides given in low letters indicate paralogous sequence variants (PSVs) between *SUZ12* and *SUZ12P*. Hyphens indicate deletions between *SUZ12* and *SUZ12P*, whereas underlined nucleotides represent insertions with respect to the paralogous sequence.

John Wiley & Sons, Inc.

Supplementary Table S4: Investigation of mosaicism with normal cells and cells harbouring the type-2 deletion in 18 NF1 patients

Patient	Sex (age in (years)	Mosaicism detected by marker analysis [a] of		Proportion (%) of cells harbouring the deletion as determined by FISH analysis of				
		blood	buccal cells	blood	buccal cells	skin fibroblast cultures	neuro-fibroma	urine
811-M[b]	f (35)	yes	—	93	—	—	—	—
KCD[c]	f (34)	yes	—	92	—	51	—	—
697[b]	f (11)	no	—	97	59	—	—	—
736[b]	f (68)	yes	—	94	59	—	—	—
1630[b]	f (15)	yes	—	92	—	—	—	—
2358[d]	f (10)	no	no	100	—	—	—	—
585[d]	f (7)	yes	yes	—	—	—	—	—
488[b]	f (33)	no	—	98	56	—	—	—
1502[b]	f (26)	no	yes	97	70	—	—	—
1956[d]	m (9)	yes	—	92	—	—	—	—
IL39[c]	f (60)	yes	—	70	—	15	—	—
1104[b]	f (36)	yes	—	84	8	—	—	15
928[b]	f (39)	no	—	100	55	—	80	—
2429[d]	m (16)	no	no	100	—	—	—	—
WB[c]	f (65)	no	—	94	—	—	—	—
938[a]	f (35)	yes	—	91	80	—	—	—
HC[a]	m (9)	no	yes	100	—	—	—	—
UC172[d]	f (6)	yes	—	86	—	—	—	—

a: mosaicism was investigated by microsatellite marker analysis and putative heterozygosity of markers located within the deletion interval using DNA isolated from peripheral blood samples (primary blood cells) and not from lymphoblastoid cell lines.
b: as determined in Steinmann et al., [2007]
c: as determined in Kehrer-Sawatzki et al., [2004]
d: as determined in this study
—: not determined

Supplementary Table S5: Results of the SNP array analysis using DNA isolated from uncultivated blood cells of 16 patients with type-2 *NF1* deletions. Heterozygous SNPs are indicated as (+), homozygous SNP are assigned as (-)

SNP	Position[a]	Array results observed in patient															
		811-M	KCD	697	736	1630	2358	585	488	1502	1956	IL39	1104	928	WB	UC172	938
rs7222696	24,721,745	+	-	-	-	-	+	-	-	-	+	-	+	+	-	-	-
rs2138852	24,727,475	+	-	-	-	-	+	-	+	-	+	+	+	-	-	-	+
rs12449974	24,731,012	-	-	-	-	-	-	-	+	-	-	+	-	+	-	-	+
rs4794854	24,749,129	+	+	-	-	-	+	-	-	-	-	-	+	-	-	-	-
rs11651087	24,761,030	-	+	-	-	-	-	-	+	-	+	+	-	-	-	-	+
rs11654359	24,761,045	-	+	-	-	-	-	-	+	-	+	+	-	-	-	-	+
rs12602428	24,764,399	+	-	-	-	-	-	-	-	-	-	-	+	+	-	-	-
rs9906280	24,771,580	+	+	-	-	-	+	-	-	-	-	-	+	-	-	-	-
rs17225878	24,803,564	+	-	-	-	-	-	-	-	-	-	-	+	+	-	-	-
rs6505138	24,833,230	+	-	-	-	-	-	-	-	-	-	-	+	+	-	-	-
rs559972	24,838,622	+	-	-	-	-	+	-	+	-	+	+	+	-	-	-	+
rs8081085	24,891,441	-	-	-	-	-	-	-	+	-	-	+	-	+	-	-	+
rs17766675	24,895,151	-	+	-	-	-	-	-	+	-	+	+	-	-	-	-	+
rs11868722	24,908,731	-	+	-	-	-	-	-	+	-	+	+	-	-	-	-	+
rs636000	24,915,990	+	-	-	+	+	-	-	-	+	-	-	-	-	-	+	+
rs550818	24,926,101	-	+	+	+	+	-	+	+	-	-	-	+	+	-	+	-
rs894606	24,933,478	+	+	-	-	-	-	-	-	+	-	-	+	+	-	-	+
rs3744626	24,935,683	-	-	+	+	+	-	+	+	+	-	-	-	-	-	+	-
rs1017529	24,936,541	-	-	-	-	+	-	-	-	+	-	-	-	-	-	-	+
rs3115094	24,937,933	-	-	-	+	+	-	+	+	-	-	-	+	+	-	+	-
rs3110496	24,941,897	-	+	-	+	+	-	-	-	-	+	-	+	+	-	+	-
rs3809789	24,979,887	-	+	+	-	+	-	+	-	-	+	-	+	-	-	-	+
rs2289629	24,984,029	-	+	+	+	+	-	+	+	-	+	-	+	-	-	-	-

For Peer Review

rs4794859	24,986,519	-	+	+	-	+	-	+	-	-	+	-	+	-	-	-	+
rs3110495	25,002,581	-	+	+	-	-	-	+	-	-	+	-	+	-	-	-	+
rs3098949	25,002,820	-	+	+	+	-	-	+	-	-	+	-	+	-	-	-	+
rs3115092	25,060,476	-	+	+	+	-	-	+	-	-	+	-	+	-	-	-	+
rs2874505	25,062,049	-	+	+	+	-	-	+	-	-	+	-	+	-	-	-	+
rs2617881	25,087,401	-	+	+	-	-	-	+	-	-	+	-	+	-	-	-	+
rs2617874	25,109,298	-	+	+	-	-	-	+	-	-	+	-	+	+	-	-	+
rs2617875	25,114,150	-	+	+	-	-	-	+	-	-	+	-	+	+	-	-	+
rs11654222	25,123,086	-	+	-	-	-	-	-	-	-	+	-	+	-	-	-	-
rs2628165	25,145,292	-	+	+	-	-	-	+	-	-	+	-	+	-	-	-	+
rs4474741	25,172,243	-	+	+	-	-	-	+	-	-	+	-	+	-	-	-	+
rs17226179	25,192,699	-	+	+	-	-	-	+	-	-	+	-	+	-	-	-	+
rs7223455	25,196,483	-	-	+	-	+	-	-	-	-	-	-	-	-	-	-	+
rs4294865	25,229,862	-	+	+	-	-	-	+	-	-	+	-	+	+	-	-	+
rs6505145	25,273,428	-	-	+	-	+	-	-	-	-	-	-	-	-	-	-	-
rs4598962	25,318,074	-	+	+	+	-	-	+	-	-	+	-	+	-	-	-	+
rs9897794	25,320,453	-	+	+	+	-	-	+	-	-	+	-	+	-	-	-	+
rs12150261	25,344,599	-	+	+	-	-	-	+	-	-	+	-	+	-	-	-	+
rs12939344	25,352,945	-	+	+	+	-	-	+	-	-	+	-	+	-	-	-	+
rs9902453	25,373,221	-	+	+	+	-	-	+	-	-	+	-	+	-	-	-	+
rs7213462	25,413,702	-	+	-	+	+	-	+	+	-	+	-	+	-	-	+	-
rs4465650	25,420,847	-	+	+	+	-	+	+	-	-	-	-	+	-	-	-	+
rs9906340	25,423,103	-	+	+	+	-	-	+	-	-	+	-	+	-	-	-	+
rs6505162	25,468,309	-	+	+	+	-	-	+	-	-	+	-	+	-	-	-	+
rs4429345	25,482,231	-	+	+	+	-	-	+	-	-	+	-	+	-	-	-	+
rs11080118	25,499,505	-	+	+	+	-	-	+	-	-	+	-	+	-	-	-	+
rs9902340	25,500,584	-	+	+	+	-	-	+	-	-	+	-	+	-	-	-	+
rs7221154	25,529,150	-	+	+	+	-	-	+	-	-	+	-	+	-	-	-	+

For Peer Review

rs2054846	25,531,819	-	+	+	+	-	-	+	-	-	+	-	+	-	-	-	+
rs1906451	25,539,605	-	+	+	+	-	-	+	-	no Call	+	-	+	-	-	-	+
rs7224199	25,547,852	-	+	+	+	-	-	+	-	-	+	-	+	no Call	-	-	+
rs140701	25,562,658	-	+	+	+	-	-	+	-	-	+	-	+	+	-	-	+
rs4583306	25,562,841	-	+	+	+	-	-	+	-	-	+	-	+	+	-	-	+
rs8076005	25,571,336	-	-	+	-	+	-	-	-	-	-	-	-	-	-	-	+
rs11080122	25,571,461	-	-	+	-	+	-	-	-	-	-	-	-	-	-	-	+
rs2020939	25,574,858	-	+	+	+	-	-	+	-	-	+	-	+	+	-	-	+
rs2020936	25,574,940	-	-	+	-	+	-	-	-	-	-	-	-	-	-	-	+
rs16965628	25,579,551	-	-	+	-	-	-	-	+	-	-	-	-	-	-	-	-
rs7214991	25,596,486	+	+	+	+	+	-	+	+	+	+	-	-	+	-	-	+
rs1050565	25,600,202	+	+	-	+	+	-	+	+	+	+	-	-	+	-	-	+
rs7223821	25,603,446	+	+	-	+	+	-	+	+	+	+	-	-	+	-	+	+
rs17767256	25,605,169	+	+	-	+	+	-	+	+	+	+	-	-	+	-	-	+
rs16965656	25,615,876	-	-	+	-	-	-	-	-	-	-	-	-	-	-	-	-
rs7209807	25,627,320	-	-	+	-	-	-	-	-	-	-	-	-	-	-	-	-
rs8072345	25,628,415	+	+	+	+	+	-	+	-	+	+	-	+	+	-	-	-
rs8081598	25,666,506	-	-	-	-	-	-	-	-	-	-	-	-	-	-	-	-
rs3110452	25,671,878	+	+	-	+	+	-	+	+	+	+	-	-	+	-	-	+
rs6505178	25,688,181	+	+	-	-	+	-	+	+	+	+	-	-	+	-	-	+
rs8079175	25,691,408	+	+	-	-	+	-	+	+	+	+	-	-	+	-	-	+
rs8068438	25,692,866	+	+	-	-	+	-	+	+	+	+	-	-	+	-	-	+
rs8082169	25,700,653	-	-	-	-	-	-	-	-	-	-	-	-	-	-	-	-
rs7215966	25,711,322	+	+	-	-	+	-	+	+	+	+	-	-	+	-	-	+
rs16965693	25,711,818	-	-	-	-	-	-	-	-	-	-	-	-	+	-	-	-
rs4794869	25,715,226	-	-	-	-	-	-	-	-	-	-	-	-	-	-	-	-
rs12952168	25,723,214	+	+	-	-	-	-	+	-	-	+	-	+	+	+	-	-
rs17803815	25,728,007	-	-	-	-	-	-	-	+	-	-	-	+	-	-	-	+

For Peer Review

rs12453652	25,754,986	+	+	-	-	-	-	+	-	-	+	-	+	+	+	-	-
rs719601	25,755,541	+	+	-	-	-	-	+	-	-	+	-	+	+	+	-	-
rs4794873	25,772,478	-	-	-	-	+	-	-	-	+	-	-	-	-	-	-	-
rs6505188	25,808,508	+	+	-	+	-	-	+	+	-	+	-	-	+	+	+	+
rs10491108	25,817,443	-	-	-	-	-	-	-	+	-	-	-	+	-	-	-	+
rs9406	25,818,146	+	+	-	-	-	-	+	+	-	+	-	-	+	+	-	+
rs9303633	25,831,576	+	+	-	-	-	-	+	+	-	+	-	-	+	+	-	+
rs9897725	25,889,787	-	-	-	-	-	-	-	+	-	-	-	+	-	-	-	+
rs216475	25,890,095	+	+	-	-	-	-	+	+	-	+	-	-	+	+	-	+
rs9898690	25,892,465	-	-	-	-	-	-	-	+	-	-	-	+	-	-	-	+
rs216480	25,892,855	+	+	-	-	-	-	+	+	-	+	-	-	+	+	-	+
rs216481	25,893,195	+	+	-	-	-	-	+	-	-	+	-	+	+	+	-	-
rs216483	25,894,853	-	+	-	-	-	-	+	-	-	+	-	+	+	+	-	-
rs216485	25,896,751	-	+	-	-	-	-	+	-	-	+	-	+	+	+	-	-
rs216450	25,902,943	-	+	-	-	-	-	+	+	-	+	-	-	+	+	-	-
rs216459	25,917,773	-	+	-	-	-	-	+	+	-	+	-	-	+	+	+	-
rs216460	25,917,804	-	+	-	-	-	+	+	+	-	-	-	+	-	+	+	-
rs17606460	25,923,150	-	+	-	-	+	-	-	+	+	+	-	-	+	-	-	-
rs216412	25,927,520	-	-	-	-	-	-	-	-	+	-	-	-	-	-	+	-
rs122898	25,929,380	-	-	-	-	-	-	-	-	+	-	-	-	-	-	+	-
rs216443	25,955,997	-	-	-	-	-	-	-	-	+	-	-	-	-	-	+	-
rs423151	25,976,412	-	-	-	-	-	-	-	-	+	-	-	-	-	-	+	-
rs9904033	26,024,145	-	+	-	-	-	-	+	+	-	+	-	+	-	-	+	+
rs8081187	26,040,486	-	-	-	-	-	-	-	+	-	-	-	+	-	-	+	+
rs11657662	26,100,473	-	-	-	-	-	-	-	-	+	-	-	-	-	-	+	-
rs9898084	26,106,460	-	-	-	-	-	-	-	-	+	-	-	-	-	-	+	-
rs9895785	26,131,834	-	-	-	-	-	-	-	-	-	-	-	-	+	-	+	-
rs7214570	26,171,290	-	-	-	-	-	-	-	-	-	-	-	-	-	-	+	-

For Peer Review

rs9912440	26,172,898	-	-	-	-	-	-	-	-	-	-	-	-	-	-	+	-
rs9915139	26,182,641	-	-	-	-	-	-	-	-	-	-	-	-	-	-	-	-
rs3816780	26,185,484	-	-	-	-	-	-	+	-	-	-	-	-	-	-	+	-
rs11080134	26,185,629	-	-	+	-	-	-	-	-	+	+	-	-	-	-	-	-
rs9890032	26,190060	-	-	-	-	-	-	-	-	-	-	-	-	-	-	-	-
rs11657270	26,238,513	-	-	-	-	-	-	+	-	-	-	-	-	-	-	+	-
rs9914242	26,240,371	-	-	-	-	-	-	+	-	-	-	-	-	-	-	+	-
rs9889755	26,258,631	-	-	-	-	-	-	+	-	-	-	-	-	-	-	+	-
rs9911989	26,261,828	-	-	-	-	-	-	+	-	-	-	-	-	-	-	+	-
rs7225461	26,284,025	-	-	-	-	-	-	-	-	-	-	+	-	-	-	-	-
rs6505219	26,289,747	+	-	-	-	-	-	-	-	-	-	-	-	-	-	+	-
rs2232281	26,307,729	-	-	-	-	-	-	-	-	-	-	-	-	-	-	-	-
rs17826255	26,357,642	+	+	-	+	+	+	+	+	+	+	+	+	+	+	+	-
rs9900686	26,360,463	-	-	-	-	-	-	-	-	-	+	-	-	-	-	-	-
rs11657989	26,419,872	-	+	-	-	-	-	-	-	-	-	-	-	-	-	-	-
rs7217921	26,420,423	-	+	-	-	-	-	-	-	-	-	-	-	-	-	-	+
rs8076441	26,430,004	+	+	+	-	+	+	+	+	+	+	+	+	+	+	-	+
rs12603885	26,490,848	-	-	-	-	-	-	-	-	-	-	-	-	-	-	-	-
rs1124918	26,516,549	-	-	-	+	-	-	+	+	+	-	-	-	-	-	+	-
rs2953013	26,520,469	-	+	-	-	-	-	-	-	+	-	-	-	-	-	-	-
rs1801052	26,532,901	-	-	-	-	-	-	-	-	-	-	-	-	-	-	-	-
rs1013948	26,554,835	-	-	+	-	-	-	-	-	+	-	-	-	-	-	-	-
rs1034705	26,560,259	+	-	-	+	+	+	+	+	-	+	+	+	+	+	+	+
rs2905877	26,567,395	-	+	+	-	-	-	-	-	+	-	-	-	-	-	-	-
rs2905880	26,570,301	-	+	-	-	-	-	-	-	-	-	-	-	-	-	-	-
rs7215555	26,588,729	-	-	-	-	+	+	+	+	-	-	+	+	-	+	-	+
rs9303642	26,602,486	-	+	-	-	-	-	-	-	+	-	-	-	-	-	-	-

rs11870910	26,626,536	+	-	-	+	-	-	-	-	-	-	-	-	-	-	-	-
rs11080149	26,647,414	-	+	-	-	-	-	-	-	-	-	-	-	-	-	-	-
rs11655238	26,648,301	-	-	-	-	-	-	-	-	-	-	-	-	-	-	-	-
rs2040792	26,652,675	+	-	+	-	-	-	-	-	+	-	-	-	-	-	-	-
rs10512434	26,663,716	+	-	+	-	+	+	-	-	+	+	+	+	+	+	-	+
rs2189525	26,692,934	-	-	-	-	-	-	+	+	-	-	-	-	-	-	+	-
rs7405740	26,694,316	+	-	-	+	-	-	-	-	-	-	-	-	-	-	-	-
rs2854311	26,695,453	-	-	-	-	-	-	-	-	-	-	-	-	-	-	-	-
rs2854322	26,723,542	-	-	-	-	-	-	-	-	+	-	-	-	-	-	-	-
rs8067440	26,732,281	-	-	-	-	-	-	-	-	-	-	-	-	-	-	-	-
rs2525578	26,735,537	-	-	+	-	-	-	-	-	+	-	-	+	-	-	-	-
rs757378	26,746,745	-	-	-	-	-	-	-	-	-	-	-	-	-	-	-	-
rs731759	26,746,935	+	-	-	-	+	-	-	-	-	-	+	+	+	-	-	+
rs735053	26,766,853	-	-	-	-	-	-	-	-	-	-	-	-	-	-	+	-
rs7218430	26,773,570	-	+	-	-	-	-	-	-	-	-	-	-	-	-	+	-
rs12941005	26,779,135	-	-	-	-	-	-	-	-	-	-	-	-	-	-	-	-
rs733276	26,786,518	-	-	-	-	-	-	-	-	+	-	-	-	-	-	-	-
rs12951187	26,791,212	-	-	-	-	-	-	-	-	-	-	-	-	-	-	-	-
rs178853	26,791,321	-	-	-	-	-	-	-	-	-	-	-	-	-	-	-	-
rs7502433	26,809,334	+	-	-	-	-	+	-	-	-	+	-	-	-	-	-	-
rs4327103	26,809,496	-	-	+	-	-	-	-	-	-	-	-	-	-	-	-	-
rs178886	26,818,596	-	+	-	-	-	-	-	-	-	-	-	-	-	-	+	-
rs4794889	26,819,348	-	-	+	-	-	-	-	-	-	+	-	-	-	-	-	-
rs11868735	26,820,323	-	-	+	-	-	-	-	-	-	+	-	-	-	-	-	-
rs178889	26,820,440	+	-	-	+	+	-	+	-	-	-	+	+	+	+	-	+
rs9909944	26,853,742	-	-	-	-	-	-	-	-	-	-	-	-	-	-	-	-
rs9901597	26,853,794	-	-	-	-	-	-	-	-	+	-	-	-	-	-	+	-

rs2343244	26,858,750	-	-	-	-	-	-	-	-	-	-	-	+	-	-	-	-
rs9908879	26,859482	-	-	-	-	-	-	-	-	-	-	-	-	+	-	-	+
rs882545	26,862,502	-	-	-	-	-	-	-	-	-	-	-	-	-	-	-	-
rs2023795	26,876,212	+	-	+	-	+	-	-	-	-	+	-	+	+	+	+	+
rs12602681	26,879,455	-	-	-	-	-	-	-	-	-	-	-	-	-	-	-	-
rs2074150	26,880,052	-	-	+	-	-	-	-	-	+	-	+	-	-	-	-	-
rs2074151	26,881,062	-	-	-	-	-	-	-	-	-	-	-	-	-	-	-	-
rs4795616	26,892,260	-	-	-	-	-	-	+	-	+	-	+	-	-	-	+	-
rs2018971	26,896,751	-	-	-	-	-	-	-	-	-	-	-	-	-	-	-	-
rs7216082	26,914,065	-	-	+	-	-	-	-	-	-	-	-	-	-	-	+	-
rs223143	26,927,449	-	-	+	-	-	-	-	-	-	-	-	+	-	-	-	-
rs17181665	26,932,784	-	-	-	-	-	-	-	-	-	-	-	-	-	-	-	-
rs1020628	26,935,918	+	-	-	-	+	-	-	-	-	-	-	-	-	-	-	+
rs8069530	26,939,821	-	+	-	+	+	-	-	-	+	-	-	+	+	+	+	-
rs17181735	26,945,053	-	-	-	-	-	-	-	-	-	-	-	-	-	-	-	-
rs192001	26,955,139	-	-	-	-	+	+	-	-	-	-	-	-	-	-	-	-
rs11080162	26,961,108	-	-	-	-	-	-	-	-	-	-	+	-	+	-	-	-
rs710962	26,963,489	-	+	+	-	-	-	-	-	-	-	-	-	-	-	+	-
rs315429	26,966,079	-	-	-	-	-	-	-	-	-	-	-	-	-	-	-	-
rs812776	26,977,514	-	-	-	-	-	-	-	-	-	-	-	-	-	-	-	+
rs167564	26,980,258	+	+	+	+	-	-	-	-	+	-	-	-	-	-	+	-
rs430432	26,989,426	-	-	-	-	-	-	-	-	-	-	-	-	-	-	-	+
rs407713	26,990,364	-	-	-	-	-	-	-	-	-	-	-	-	-	-	-	-
rs770497	26,997,435	-	-	-	-	+	-	-	-	-	+	+	+	+	+	-	-
rs16972368	27,000,763	-	-	-	-	-	-	-	-	-	-	-	-	-	-	-	-
rs770520	27,004,572	+	-	+	-	+	+	-	-	+	+	+	+	+	+	-	+
rs770521	27,004,671	+	-	-	-	+	+	-	-	+	+	+	+	+	+	-	-

rs315431	27,005,299	-	-	-	-	-	-	-	-	-	-	-	-	-	-	-	-
rs315437	27,007,946	-	-	-	-	-	+	-	-	-	-	-	-	-	-	-	-
rs315439	27,009,191	-	-	-	+	-	-	-	-	-	-	-	-	-	-	+	+
rs373531	27,011,628	-	-	-	-	-	-	-	-	-	-	-	-	-	-	-	-
rs12936664	27,024,408	+	-	-	-	-	-	+	-	+	+	-	+	-	-	-	-
rs447750	27,024,517	-	+	+	-	-	-	-	+	-	-	-	-	-	-	-	-
rs9893718	27,025,948	-	-	+	-	-	-	-	+	-	-	-	+	-	-	-	-
rs9893975	27,026,066	-	-	-	-	-	-	-	-	-	-	-	-	-	-	-	-
rs425083	27,028,247	-	-	+	+	-	-	+	-	-	-	-	-	-	-	+	-
rs427272	27,029,068	-	-	-	-	-	-	-	-	-	-	-	-	-	+	+	+
rs425967	27,038,309	-	+	-	+	-	-	-	-	-	-	-	-	-	+	+	+
rs385559	27,038,826	-	+	-	+	+	-	-	-	-	-	-	-	-	+	+	+
rs421875	27,041,382	-	+	-	+	-	-	-	-	-	-	-	-	+	+	+	+
rs11658518	27,047,758	-	-	-	-	-	-	-	-	-	-	-	-	-	-	-	-
rs7222438	27,057,935	-	-	-	-	-	+	-	-	+	-	-	-	-	-	-	-
rs16966835	27,060,691	-	-	-	-	-	-	-	-	-	-	+	-	-	-	-	-
rs315495	27,060,818	-	-	-	-	-	-	-	-	-	-	-	-	-	-	-	-
rs9890598	27,061,309	-	-	-	-	-	-	-	-	-	-	-	-	-	-	-	-
rs9898609	27,061,818	-	-	-	-	-	-	-	-	-	-	-	-	-	-	-	-
rs315502	27,062,713	+	-	-	-	-	-	+	-	-	-	-	-	+	-	+	-
rs17182078	27,072,868	-	-	-	-	-	-	-	-	-	-	-	-	-	-	-	-
rs884351	27,073,028	-	-	-	-	-	-	-	-	-	+	-	+	-	-	-	-
rs8066501	27,075,820	-	-	+	-	-	-	-	+	-	-	-	+	-	-	+	-
rs12939349	27,076,025	-	+	-	+	-	-	-	-	-	-	-	-	-	-	-	+
rs2111662	27,079,871	-	+	-	-	+	-	-	-	-	-	-	-	-	-	-	-
rs16966855	27,088,333	-	-	-	-	-	-	-	-	-	-	-	-	-	-	-	-
rs17827108	27,088,517	-	-	-	+	-	-	-	-	+	+	-	-	-	-	-	+

rs16966858	27,088,939	-	-	+	-	-	-	-	-	-	-	-	-	-	-	-	-
rs17246714	27,089,201	-	-	-	-	-	-	-	-	-	-	-	-	-	-	-	-
rs9914500	27,091,540	-	-	-	-	-	-	-	-	-	-	-	-	-	-	-	-
rs8074803	27,093,316	-	-	-	-	-	-	-	-	-	-	-	-	-	-	-	-
rs11871038	27,094,989	-	-	-	-	-	-	-	-	-	-	-	-	-	-	-	-
rs2111666	27,102,412	-	-	-	+	-	-	-	-	-	-	-	-	-	-	-	-
rs9910565	27,109,313	-	-	-	-	+	+	-	-	-	-	-	+	-	+	-	+
rs8066989	27,109,945	-	-	-	-	-	+	-	-	-	-	-	-	-	-	-	-
rs11651399	27,129,435	-	-	-	-	-	-	-	-	-	-	-	-	-	-	-	-
rs9902100	27,138,441	+	+	+	-	+	+	-	+	+	-	+	+	+	+	+	-
rs13380855	27,139,087	-	-	-	-	-	-	+	-	-	-	-	-	-	-	-	-
rs9898619	27,141,418	-	-	-	-	-	-	-	-	-	-	-	-	-	-	-	-
rs16966942	27,144,777	-	-	-	-	-	-	-	-	+	-	-	-	-	-	-	-
rs11080170	27,145,874	-	-	-	-	-	-	-	-	-	-	-	-	-	-	-	-
rs9905200	27,147,900	-	-	-	-	-	-	+	-	-	-	-	-	-	-	-	-
rs757288	27,148,090	+	-	+	+	+	-	+	+	+	+	+	+	+	+	+	+
rs757289	27,148,193	-	+	+	+	-	-	+	-	+	+	-	-	+	-	-	-
rs4795653	27,163,735	-	+	+	+	-	-	-	-	+	+	-	-	+	-	-	-
rs1468263	27,171,997	-	-	-	-	-	-	-	-	-	-	-	-	-	-	-	-
rs8068039	27,182,757	-	-	-	-	-	-	-	-	-	-	-	-	-	-	-	-
rs8074024	27,182,912	-	-	-	-	-	-	-	-	-	+	-	-	+	-	-	+
rs4795658	27,185,863	-	-	-	-	-	-	-	-	-	-	-	-	-	-	-	-
rs6505265	27,196,693	-	-	+	-	-	-	-	-	-	-	-	-	-	-	-	-
rs7223225	27,197,449	-	-	-	-	-	-	-	-	-	-	-	-	-	-	-	-
rs16967012	27,198,077	-	-	-	-	-	-	-	-	+	-	-	-	-	-	+	-
rs2344310	27,205,319	-	+	-	+	-	-	+	-	+	-	-	-	+	-	+	-
rs12941700	27,209,135	+	-	-	-	+	+	+	+	+	+	+	+	-	-	+	+

rs9906443	27,209,678	-	-	-	-	-	-	-	-	-	+	-	-	-	-	-	-
rs9899093	27,216,067	-	-	-	-	-	-	-	-	-	-	-	-	-	-	-	-
rs16967029	27,219,405	-	-	-	-	-	-	-	-	-	-	-	-	-	-	+	-
rs7209493	27,221,436	-	-	-	-	-	-	-	-	-	-	-	-	-	-	-	-
rs8079471	27,242,430	-	-	-	-	-	-	-	-	-	-	-	-	-	-	-	-
rs1034626	27,243,613	-	-	-	-	-	-	-	-	-	-	-	-	-	-	-	-
rs1034627	27,243,682	-	-	+	-	-	-	-	-	+	+	-	+	-	-	-	-
rs3760454	27,246,115	-	-	-	-	-	-	-	-	-	-	-	-	-	-	-	-
rs7222814	27,248,984	-	-	-	-	-	-	-	-	+	-	-	-	-	-	-	-
rs7216102	27,283,563	-	-	-	-	-	-	-	-	-	-	-	-	-	-	-	-
rs578635	27,314,010	-	+	-	+	-	+	-	-	+	+	+	+	-	+	+	-
rs501957	27,338,617	-	+	-	+	-	-	-	-	-	-	-	-	+	-	-	-
rs508192	27,339,260	-	+	+	+	-	-	-	-	-	-	-	-	+	-	-	-
rs497479	27,352,718	-	+	-	+	-	-	-	-	-	-	-	-	+	-	-	-
rs8066156	27,385,742	-	+	-	+	-	-	-	-	-	-	-	-	+	-	-	-
rs8076067	27,460,756	-	+	-	+	+	-	-	-	-	-	-	-	+	-	-	+
rs7212461	27,470,861	-	+	-	+	+	-	-	-	-	-	-	-	+	-	-	+
rs7210088	27,474,705	-	+	-	+	+	-	-	-	-	-	-	-	+	-	-	+
rs1993791	27,525,515	-	+	-	+	+	-	-	-	-	-	-	-	+	-	-	+
rs1993790	27,525,531	-	+	-	+	+	-	-	-	-	-	-	-	+	-	-	+
rs2036376	27,558,424	-	+	-	+	+	-	+	-	-	-	-	-	+	-	-	+
rs7216187	27,568,352	-	+	-	+	+	-	-	-	-	-	-	-	+	-	-	+
rs9902253	27,573,486	-	+	-	+	+	-	-	-	-	-	-	-	+	-	-	+
rs17182658	27,573,557	-	-	-	-	-	-	-	-	-	-	-	-	-	-	-	-
rs16967213	27,580,395	-	+	-	+	+	-	-	-	-	-	-	-	+	-	-	+
rs3744616	27,593,261	-	-	-	-	-	-	-	-	-	-	-	-	-	-	-	-
rs12944565	27,604,385	-	+	-	-	-	-	-	+	-	+	+	-	+	+	+	-
rs12452958	27,605,972	-	-	-	-	-	-	-	-	-	-	-	-	-	+	-	-

For Review

rs12325966	27,606,107	+	-	-	-	-	-	-	-	-	+	-	+	-	+	+	-
rs1039402	27,610,212	+	-	-	-	-	-	-	-	-	+	-	+	-	+	+	-
rs726502	27,612,377	+	-	-	-	+	-	-	+	-	-	+	+	+	-	-	-
rs12453610	27,619,952	+	-	-	-	+	-	-	+	-	+	+	+	+	-	-	-
rs9907164	27,620,126	-	+	-	-	-	-	-	-	-	+	+	-	+	+	+	-
rs4795686	27,620,615	-	+	-	-	-	-	-	-	-	+	+	-	+	+	+	-
rs5002530	27,622,256	+	-	-	-	+	-	-	+	-	+	+	-	+	-	-	+
rs1530381	27,626,251	+	-	-	-	+	-	-	+	-	+	+	+	+	-	-	-
rs17780388	27,630,414	+	+	-	-	+	-	-	+	-	-	-	+	-	+	+	-
rs16967244	27,636,926	+	+	-	-	+	-	-	+	-	-	-	-	-	+	+	-
rs17732573	27,651,777	-	-	-	-	+	-	+	+	-	+	+	-	-	+	+	-
rs4794915	27,658,476	-	+	-	-	+	-	+	-	-	+	+	+	+	-	+	-
rs1019152	27,683,119	-	+	-	-	-	-	-	-	+	+	+	-	-	-	+	-
rs8069673	27,685,363	-	+	-	-	+	+	+	-	+	+	+	+	+	-	+	-
rs9904964	27,686,945	-	+	-	-	+	-	+	-	+	+	+	+	+	-	+	-
rs9901737	27,705,467	-	+	-	-	+	-	+	-	+	+	+	+	+	-	+	-
rs3795244	27,716,509	-	+	-	-	-	-	-	-	-	-	-	+	+	-	-	-
rs2344977	27,744,686	-	-	-	-	+	-	+	+	+	+	+	-	-	+	+	-
rs8070777	27,789,577	-	+	-	-	-	-	-	+	-	-	-	+	+	+	-	-
rs9910731	27,808,147	-	+	-	-	+	-	+	+	+	-	+	+	+	-	+	-
rs9889607	27,809,698	-	+	-	-	+	-	+	+	+	-	+	+	+	-	+	-
rs12162135	27,829,908	-	-	-	-	+	-	-	+	+	-	+	-	-	+	+	-
rs735555	27,841,563	-	-	-	-	+	-	+	-	+	+	+	-	-	+	+	-
rs731880	27,842,822	-	+	-	-	-	-	-	+	-	-	-	+	-	+	-	-
rs2285428	27,844,289	-	+	-	-	+	-	+	+	+	-	+	+	+	-	+	-
rs9889771	27,847,120	+	+	-	+	+	-	-	+	-	-	-	+	+	+	-	-
rs1018866	27,853,777	-	-	-	-	-	-	+	+	+	+	+	-	-	+	+	-
rs17806303	27,855,741	-	-	-	-	-	-	-	-	+	-	-	-	-	-	-	-

For Peer Review

rs916663	27,859,946	+	-	-	-	+	-	+	-	+	+	-	-	-	+	+	-
rs17806429	27,882,512	+	-	-	-	-	-	-	-	-	-	-	-	-	-	-	-
rs2706755	27,883,082	-	-	-	+	-	-	+	-	-	+	-	-	-	-	-	+
rs1034593	27,885,978	+	+	-	+	-	+	+	+	-	+	-	-	-	-	+	+
rs6505300	27,894,053	+	+	-	+	-	+	+	+	-	+	-	-	-	-	+	+
rs2519861	27,895,953	+	-	+	+	-	+	+	-	-	-	+	-	-	-	-	-
rs4794928	27,896,684	-	+	-	-	-	-	-	-	-	+	-	-	-	-	-	-
rs1989805	27,897,975	+	-	+	+	-	+	+	-	-	+	+	-	-	-	-	-
rs225188	27,902,283	+	+	+	+	-	+	+	-	-	+	+	-	-	-	-	-
rs9903536	27,902,861	+	+	+	+	-	+	-	+	-	+	+	-	-	-	+	-
rs9890602	27,904,495	-	-	-	-	-	-	-	-	-	-	-	-	-	-	+	-
rs225186	27,905,012	-	+	+	+	-	-	+	+	+	-	+	+	+	-	+	+
rs225184	27,906,240	+	-	+	+	+	-	-	+	-	-	-	+	-	+	-	-
rs389774	27,909,678	+	-	+	+	+	-	-	+	-	-	-	+	-	+	-	-
rs11657700	27,917,684	+	+	+	-	-	+	+	+	-	-	+	-	+	+	-	-
rs225205	27,918,399	+	-	+	+	-	+	+	+	-	-	+	-	-	+	-	-
rs225206	27,918,485	-	-	+	+	-	+	+	+	-	-	+	-	-	+	+	-
rs225207	27,918,837	+	-	+	+	+	-	-	+	-	-	-	+	-	+	-	-
rs225209	27,918,999	-	-	+	+	-	+	+	+	-	-	+	-	-	+	+	-
rs225211	27,919,415	+	-	+	+	-	+	+	+	-	-	+	-	-	+	-	-
rs6505303	27,,919,727	-	-	-	-	+	+	+	-	-	-	+	+	-	-	-	-
rs225212	27,920,568	+	-	+	+	-	+	+	+	-	-	+	-	-	+	-	-
rs225214	27,920,869	+	-	+	+	-	+	+	+	-	-	+	-	-	+	-	-
rs225215	27,921,023	-	-	+	+	-	+	+	+	-	-	+	-	-	+	+	-

a: according to the human, gen,ome assembly hg18, NCBI 36

For Peer Review

Supplementary Table S6: Position of runs of homozygosity (ROHs) ≥ 200 kb located distal to the type-2 *NF1* deletions in 13 of 16 patients investigated by SNP arrays

Patient	Position[a] of the ROH on chromosome 17		Length (bp)
	start	end	
811-M	27,314,010	27,605,972	291,962
697	27,314,010	27,894,053	580,043
736	27,593,261	27,882,512	289,251
2358	27,338,617	27,883,082	544,465
585	27,338,617	27,636,926	298,309
488	27,338,617	27,593,261	254,644
1502	27,338,617	27,658,476	319,859
1956	27,338,617	27,593,261	254,644
IL39	27,338,617	27,593,261	254,644
1104	27,338,617	27,605,972	267,355
WB	27,338,617	27,593,261	254,644
UC172	27,314,010	27,593,261	279,251
938	27,593,261	27,882,512	289,251

a: Nucleotide numbering of chromosome 17 according to hg18, NCBI build 36.1, Ensembl database version 54.36p.

For Peer Review

Supplementary Table S7: Positions of runs of homozygosity (ROHs) ≥ 200 kb located distal to the type-2 *NF1* deletion interval in 60 CEU individuals as determined by the analysis of phased haplotypes downloaded from HapMap (HapMap Data Rel 24/phaseII Nov08, on NCBI B36, assembly dbSNPb126) [Roehl et al., 2010]

CEU individuals	Position[a] of the ROH on chromosome 17		Length (bp)
	start	end	
NA06985	27,352,718	27,593,261	240,544
NA06993	27,352,718	27,580,395	227,678
NA06994	27,605,972	27,904,495	298,524
NA07000	27,352,718	27,605,972	253,255
NA07022	27,420,000	27,651,777	231,778
NA07055	27,651,777	27,853,777	202,001
NA07056	27,651,777	27,883,082	231,306
	27,352,718	27,605,972	253,255
NA07345	27,352,718	27,580,395	227,678
	27,630,414	27,909,678	279,265
NA11831	27,352,718	27,636,926	284,209
NA11832	27,352,718	27,580,395	227,678
NA11839	27,352,718	27,593,261	240,544
NA11840	27,651,777	27,883,082	231,306
	27,352,718	27,605,972	253,255
NA11881	27,352,718	27,636,926	284,209
NA11882	27,633,000	27,853,777	220,778
	27,352,718	27,580,395	227,678
NA11992	27,352,718	27,580,395	227,678
NA11995	27,651,777	27,883,082	231,306
NA12003	27,352,718	27,573,486	220,769
NA12004	27,352,718	27,593,261	240,544
NA12005	27,352,718	27,593,261	240,544
NA12006	27,352,718	27,593,261	240,544
NA12043	27,352,718	27,610,212	257,495
NA12044	27,352,718	27,580,395	227,678
NA12056	27,352,718	27,593,261	240,544
	27,605,972	27,883,082	277,111
NA12057	27,651,777	27,883,082	231,306
	27,352,718	27,605,972	253,255
NA12145	27,651,777	27,855,741	203,965
NA12146	27,352,718	27,593,261	240,544
NA12154	27,352,718	27,580,395	227,678
NA12155	27,352,718	27,883,082	530,365
NA12156	27,633,000	27,844,289	211,290
NA12236	27,352,718	27,636,926	284,209
NA12249	27,352,718	27,897,975	545,258
NA12264	27,352,718	27,593,261	240,544
NA12716	27,352,718	27,855,741	503,024

For Peer Review

NA12717	27,651,777	27,853,777	202,001
	27,352,718	27,605,972	253,255
NA12750	27,352,718	27,921,023	568,306
NA12760	27,352,718	27,580,395	227,678
NA12763	27,630,414	27,853,777	223,364
	27,352,718	27,593,261	240,544
NA12812	27,352,718	27,894,053	541,336
NA12814	27,352,718	27,605,972	253,255
NA12875	27,352,718	27,593,261	240,544
NA12892	27,352,718	27,558,424	205,707

a: Nucleotide numbering of chromosome 17 according to hg18, NCBI build 36.1, Ensembl database version 54.36p.

For Peer Review

Supplementary Table S8: Motifs identified in the recombination regions (RRs) of 16 type-2 deletions caused by NAHR between *SUZ12* and *SUZ12P*

Motif	**Consensus sequence** [a]	**Number of motifs (and their complements) identified within the RRs**
Vaccinia topoisomerase I consensus cleavage site	YCCTT	7
Immunoglobulin heavy chain class switch repeat	GAGCT, TGGGG, GGGCT,GGGGT, TGAGC	13
Chi and chi-like elements	CCWCCWGC	2*
Human minisatellite consensus sequence	GCWGGWGG	2*
Short polypurine/ polypyrimidine tracts	R_5/Y_5	16
Long polypurine/ polypyrimidine tracts	R_{10}/Y_{10}	1/2
Murine parvovirus recombination hotspot	CTWTTY	9
Deletion hotspot consensus sequence	TGRRKM	13
DNA polymerase arrest site	WGGAG	7
DNA polymerase β frameshift hotspot	ACCCWR	3
Hamster deletion hotspot sequence	TGGAG	2
Hamster and human *APRT* deletion hotspot	TTCTTC	3
Super hotspot motifs [c]	CCAAR, CCCAG AGCTG CCACCA	13 6 4 4

[a]: R=A/G, Y=C/T, W=A/T, S=G/C, M=A/C, K=G/T, N= any base. The complementary sequence was also investigated, but the corresponding sequence motifs are not listed.
* Sequences significantly overrepresented at the 5% level in RRs.

For Peer Review

Supplementary Table S9: Frequency of *Alu* elements within the recombination regions (RRs) of 16 type-2 *NF1* deletions mediated by NAHR

Patient	Position of the RR within the *SUZ12* gene	RR length (bp)	Type of *Alu* element identified within the RR (length in bp)
811-M	27,297,456-27,297,501	46	*Alu* Sx (46)
KCD	27,299,613-27,299,721	109	–
697	27,304,631-27,304,699	69	*Alu* Jo (67)
736	27,308,895-27,308,982	88	*Alu* Sz (82)
1630	27,313,160-27,313,271	112	–
2358	27,316,556-27,316,619	64	–
585	27,316,621-27,316,750	130	–
488	27,318,189-27,318,245	57	*Alu* Y (56)
1502	27,318,355-27,318,545	191	*Alu* Yc (47)
1956	27,318,916-27,319,061	146	*Alu* Jo (96)
IL39	27,322,062-27,322,108	47	–
1104	27,322,154-27,322,229	76	–
2429	27,329,593-27,329,817	225	*Alu* FLAM C (58)
WB	27,331,894-27,332,070	177	*Alu* Yk11 (54)
UC172	27,331,894-27,332,070	177	*Alu* Yk11 (54)
938	27,334,336-27,334,446	111	*Alu* Sx (41)

To determine whether *Alu* elements were overrepresented in the breakpoint regions of the 16 type-2 *NF1* deletions mediated by NAHR, the number of *Alu* sequences in the breakpoint regions was ascertained by *Repeatmasker* analysis (http://www.repeatmasker.org/cgi-bin/WEBRepeatMasker). Ten *Alu* sequences were identified in the 16 breakpoint regions with a mean length of 114 bp. The *SUZ12* gene and *SUZ12P* pseudogene are highly homologous over 45 kb as determined by BLAT analysis (http://genome.ucsc.edu/). Within this 45 kb sequence, 71 *Alu* elements were identified. Accordingly, in 1825 bp of *SUZ12* (the total length of the breakpoint regions), 2.9 *Alu* elements would be expected. However, since we observed 10 *Alu* elements in the breakpoint regions, it was concluded that *Alu* elements were significantly overrepresented at the type-2 deletion breakpoints ($p < 0.0001$; exact exact goodness-of-fit χ^2 test).

Supplementary Table S10: DNA stability, measured as ΔG° values, within the recombination regions (RR) of 14 patients with mosaic type-2 *NF1* deletions mediated by NAHR

Patient	ΔG° (kcal) of 50 bp in the centre of the RR	ΔG° (kcal) within the RR (bp)	ΔG° of a 3 kb sequence including and flanking the RR
811-M	1.94	1.94 (45)	1.78
KCD	1.75	1.75 (108)	1.79
697	1.96	1.95 (68)	1.94
736	2.04	2.03 (87)	1.94
1630	1.77	1.79 (111)	1.87
585	1.6	1.66 (129)	1.86
488	1.97	1.96 (56)	1.88
1502	1.82	1.81 (190)	1.87
1956	1.87	1.89 (145)	1.89
IL39	1.61	1.61 (46)	1.87
1104	1.63	1.63 (75)	1.86
WB	1.75	1.77 (174)	1.8
UC172	1.75	1.77 (174)	1.8
938	1.68	1.7 (110)	1.79
Mean	1.8	1.8	1.85 [95% CI: 1.82–1.88]

The DNA stability of the RRs of the type-2 *NF1* deletions was significantly lower than in the PRS1 (ΔG°: 2.008) and PRS2 (ΔG°: 2.152) hotspot regions of type-1 *NF1* deletions ($P < 0.0001$; one-sample *t*-test). CI: confidence interval assigned under the assumption of a normal distribution. The average ΔG° of the complete *SUZ12* gene is 1.871, of the *SUZ12P* pseudogene 1.877, and of the NF1-REP A 1.976.

For Peer Review

Supplementary Table S11: GC-content of the recombination regions (RRs) of the 14 type-2 *NF1* deletions mediated by NAHR during the mitotic cell cycle

Patient	GC-content of the RRs within the *SUZ12* gene (%)	GC-content of 3 kb including and flanking the RRs within the *SUZ12* gene (%)
811-M	50.0	34.8
KCD	31.2	36.6
697	56.5	46.3
736	54.6	46.3
1630	36.6	43.3
585	26.2	40.2
488	56.1	41.9
1502	41.9	42.0
1956	47.3	44.1
IL39	23.4	40.4
1104	26.3	40.8
WB	37.3	36.0
UC172	37.3	36.0
938	29.7	36.1
Mean	39.1	40.3 [95% CI: 38.1–42.6]

The GC-content of the type-2 *NF1* deletion RRs is significantly lower than the GC-content of the PRS1 (50.9%) and PRS2 (58.2%) hotspot regions of type-1 deletions ($P < 0.0001$; one-sample *t*-test). CI: confidence interval assigned under the assumption of a normal distribution. The average GC-content of the complete *SUZ12* gene is 42.6%, of the *SUZ12P* pseudogene 43.1%, and of the NF1-REP A 33.8%.

For Peer Review